MATERIALS CHEMISTRY FRONTIERS

REVIEW

View Article Online
View Journal | View Issue

Cite this: *Mater. Chem. Front.*, 2021, **5**, 584

Supramolecular gels in cyanide sensing: a review

Santanu Panja, *[a] Atanu Panja[b] and Kumaresh Ghosh *[b]

Supramolecular low molecular weight gels have potential in many areas from medicine to optoelectronics. Of the different applications, visual sensing of chemical analytes using gels is a fairly new concept in materials chemistry research. Among various analytes, cyanide is considered the most threatening to the environment and human life because of its acute toxicity. Generally, the detection of cyanide involves the use of sophisticated and expensive instrumentation, which complementary entails highly trained personnel to operate it. In contrast, a gel-based visual detection technique provides an advantage as it is simple, cost-effective, and instrument-free whilst the sensing event can be executed either by observing a phase transformation or by a naked eye detectable color change of the gel. Further, as the gel formation requires a high concentration of gelator ($\geq 10^{-3}$ M), for the same chemical compound, the gel phase interactions often exhibit better selectivity for the ionic guests than in the solution state. Despite these facts, limited attempts have been made to synthesize gel-based cyanide sensors. In this review, we discuss an up-to-date summary of various reports on cyanide responsive gels emphasizing the approaches, design principles, and reaction mechanisms. We also highlight the advantages, limitations, and challenges as well as the necessity of further exploration of gels in this domain.

Received 28th July 2020,
Accepted 8th September 2020

DOI: 10.1039/d0qm00551g

rsc.li/frontiers-materials

[a] *School of Chemistry, University of Glasgow, G12 8QQ, UK. E-mail: chem.santanu@gmail.com, santanu.panja@glasgow.ac.uk*
[b] *Department of Chemistry, Faculty of Science, University of Kalyani, Kalyani-741235, India. E-mail: ghosh_k2003@yahoo.co.in, kumareshchem18@klyuniv.ac.in; Fax: +91-3325828282; Tel: +913325828750 ext. 305*

Introduction

Low molecular weight supramolecular gels are important soft materials that draw attention in both academic and industrial research. These are formed by the self-assembly of small organic

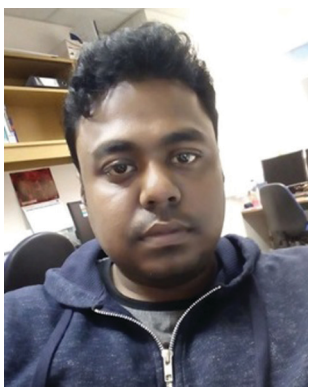

Santanu Panja

Santanu Panja received his MSc degree with specialization in organic chemistry in 2011 from the University of Calcutta, India. After qualifying for the national eligibility test (NET) jointly conducted by UGC and CSIR, Govt. of India, successively in 2010 and 2011, he joined the University of Kalyani to pursue doctoral research on supramolecular chemistry under the supervision of Prof. Kumaresh Ghosh. In 2017, he started his post-doctoral research career at the Université de Bordeaux, France, until he joined the University of Glasgow under the Newton International Fellowship program in March 2018 to work with Prof. Dave J. Adams. Presently he is associated with the same group as a research associate. He is an Associate Editorial board member of Mini Reviews in Organic Chemistry (MROC) and Current Smart Materials (CEM). His research interest covers the area of supramolecular chemistry, specifically gel chemistry.

Atanu Panja

Atanu Panja received his MSc degree with specialization in organic chemistry in 2012 from the University of Calcutta, India. He obtained his PhD in 2019 under the supervision of Prof. Kumaresh Ghosh at the University of Kalyani. His research thesis includes the design and synthesis of cation and anion responsive supramolecular gelators. Presently, he is working in TCG Lifesciences (Chembiotek), Kolkata, as a Research Scientist.

molecules leading to network structures that immobilize solvents. Despite having large amounts of liquids, these materials behave as viscoelastic solids.[1–7] The solid nature arising from the network is maintained by the tandem effects of various weak non-covalent interactions, such as hydrogen bonding, π-stacking, ionic interactions, hydrophobic interactions *etc.*[8–15] As the interactions are individually weak and reversible, it is possible to tune and control the gel properties, which enables one to explore them in many areas including catalysis, tissue engineering, and environmental remediation.[15–29]

Nowadays, there is a great deal of interest in designing 'smart gels', where the 'smart' nature arises from excellent responsiveness of the gels towards various external stimuli such as pH, light, redox, ions, ultrasound, mechanical stress *etc.*[30–42] Exposure of gels to external stimuli results in changes in molecular level interactions that bring various macroscopic changes in properties like the shape and mechanical and optical properties of gels.[43–55] Stimuli responsiveness notably extends the scope of applications of gels in the fields of sensing, actuators, drug delivery, optoelectronics *etc.*[56–79] Of the various stimuli, ionic analytes dramatically change the chemical as well as optical properties of gels[80–88] and thus there is immense scope for developing gelation-based visual sensors.[89–100] Exploitation of gels in sensing involves the interaction of the externally added ionic analytes with the gelator molecules, which produces multiple responses of gelators (Fig. 1). The most common is the destruction of the network structure, which results in gel-to-sol conversion. Alternatively, upon interaction, a change in the gel network that leads to a gel-to-gel transition can occur. Thus ion-responsive gels deserve attention not only for their attributes in visual detection of ionic analytes but also to adapt their material properties.

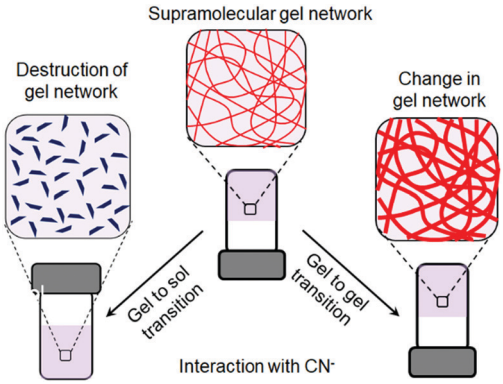

Fig. 1 Cartoon representing different modes of cyanide sensing by supramolecular gels.

Out of several ionic analytes, sensing and detection of cyanide (CN^-) ions demands considerable attention as they are considered to be the most threatening for the environment and human life.[101–103] Cyanide is mostly produced as industrial waste. It is extensively used in the textile, paper, and plastic industries as well as in gold and silver extraction processes.[104,105] Cyanide can also be released from biological processes of bacteria, fungi, and algae and even from human activity such as cigarette smoking.[105–107] However, CN^- is extremely toxic to the human body. It forms a stable complex with cytochrome *c* oxidase leading to inhibition of enzyme activity and thereby decreases the oxygen supply to the cell, which ultimately leads to cellular asphyxiation.[108,109] Accumulation of CN^- causes disorder in the nervous system and respiratory problems and eventually leads to death within a few minutes.[110,111] By considering the adverse effect of cyanide on human health, the World Health Organization (WHO) has fixed the maximum acceptable level of cyanide concentration in drinking water at 0.2 ppm.[112] Therefore, sensing and detection of cyanide ions is of utmost importance.

Generally, detection of ionic analytes is performed in the solution state at a concentration of $\leq 10^{-5}$ M by using different instrumental techniques, which show changes in absorbance, emission, surface plasmon resonance, electrochemical properties, circular dichroism *etc.*[113–126] Most of these detection techniques involve the use of sophisticated and expensive instruments and complementarily entail highly trained personnel to operate them. On the contrary, a gel-based visual detection technique provides an advantage as it is simple, cost-effective, and mostly instrument-free (in some cases a normal UV-light source is used), whilst the sensing event can be executed either by observing a phase transformation or by a naked eye detectable color change of the gel. Further, gel formation requires a high concentration of gelator ($\geq 10^{-3}$ M). In many cases, for the same chemical compound, the gel phase interactions exhibit better selectivity for the ionic guests than in the solution state.[127–131]

Scrutiny of the literature reveals that although several artificial receptors have been synthesized for sensing of CN^- ions in solution,[132–148] very few design-based molecules are explored

Kumaresh Ghosh

Dr Kumaresh Ghosh is a Professor in the Department of Chemistry, University of Kalyani, India. He did his MSc in Chemistry at the Indian Institute of Technology, Kharagpur, India, in 1994 and received his PhD degree in Supramolecular Chemistry in 1999 under the supervision of Prof. Shyamaprosad Goswami from the same institute. Prof. Ghosh was elected as a Fellow of West Bengal Academy of Science and Technology in 2017. Besides, he received the Dr Basudev Banerjee Memorial Award – 2007 (from Indian Chemical Society), Prof. D. K. Banerjee Memorial Award – 2011 (from Indian Institute of Science, Bangalore) and also CRSI Bronze Medal from the Chemical Research Society of India for the year 2018. He is an Editorial board member of Mini Reviews in Organic Chemistry. His research interests focus on supramolecular chemistry, molecular recognition, supramolecular gels and molecular probes for sensing of biologically relevant species.

for their visual detection involving supramolecular gels. This is due to a lack of understanding of the gelling behavior of gelators with proper structural parameters.[16,149–158] Additional trouble relates to the correct use of CN^--specific binding sites in the gelators to show selectivity in the sensing process. In the context of the application of self-assembled supramolecular structures, a number of reviews are available on gel-based visual detection of ionic analytes.[89–100] However, discussion on CN^- responsive gels is hardly incorporated. As the use of gels for visual detection of CN^- is a fairly new phenomenon, a detailed and up-to-date summary of work in this domain is highly demanding. From this perspective, the current review focusing on design-based CN^--responsive supramolecular gels is well-timed and long overdue.

The design strategy for CN^--responsive LMWGs

Design of small molecule-based anion responsive gelators is an important aspect of supramolecular chemistry. Anion responsive gelators typically contain an anion binding site. As the anions are basic in nature, two types of interactions are common in the gels: electrostatic interactions with oppositely charged centers (*e.g.* metal ions) and hydrogen bonding interactions with several functionalities such as hydroxyl, urea, amide, sulphonamide *etc.*[83,86,93,159–164] However, unlike other anions such as F^- and AcO^-, CN^- behaves as a good nucleophile.[134] However, its basicity and nucleophilicity strongly depend on the nature of the working solvent. Thus, depending upon the gelation conditions and binding sites, CN^--responsive gels can exhibit different types of interaction. Apart from the binding site, the rest of the gelator's backbone is manipulated with hydrophobic or hydrophilic groups of various kinds[11,152,165–174] (*e.g.*, cholesterol, long alkyl chains, amino acid derivatives, aromatic π-surfaces *etc.*) that assist self-aggregation of the molecule in solution.

Depending on the nature of the interaction, CN^--responsive gelators are broadly classified into three categories:

(i) Metal-anchored CN^- sensory gels
(ii) H-bonding motif-based CN^- sensory gels
(iii) Reaction-based CN^- sensory gelators

Herein, we summarize these three categories by giving up-to-date details. In the discussion, advantages, limitations, challenges, and future possibilities of cyanide-responsive LMWGs are also highlighted.

(i) Metal-anchored CN^- sensory gels

Organic ligands which upon coordination of metal ions show gelation involving various weak forces belong to the class of metal-anchored gelators. Gels derived from these gelators are of growing interest in materials chemistry.[41,51,96,174–176] In the present context, metal-anchored gelators draw attention because of the presence of metal ions that exhibit electrostatic interactions with anions. In designing these gelators, suitable metal ion binding sites are incorporated in the structural backbones. Generally, pyridine, acylhydrazone and salicylimine segments, *etc.* are introduced as metal ion binders. When cyanide is added externally, instead of

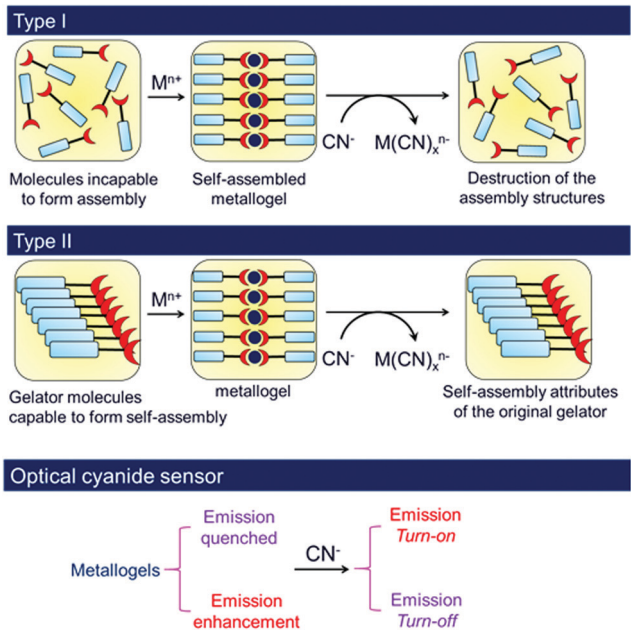

Fig. 2 Schematic representation of two different approaches (Type I and Type II) of cyanide sensing involving metal anchored gels associated with changes in emission.

interacting with the gelator, cyanide binds to the metal ion, leading to scavenging of the metal ions from the gel matrix. Depending upon the nature of the gelators, two different scenarios may appear (Fig. 2). In one case, the compound is a nongelator, but forms a gel in the presence of suitable metal ions. The scavenging of the metal ions by cyanide ions from this gel results in the collapse of the gel network, leading to a return to the solution state. In another case, if the gelator is capable of forming a self-supported gel even in the absence of the metal ion, metal displacement by cyanide drives the system to achieve the original attributes of the gelator. Consequently, a gel-to-gel transition is accomplished with a change in physicochemical properties such as the color, emission, thermal stability, mechanical properties, *etc.* of the gel (Fig. 2). Interestingly, the selectivity of metal-anchored gels towards cyanide can be controlled just by altering the nature of the metal ions.

Typical examples of Type I of Fig. 2 are compounds **1a** and **1b** reported by the Damodaran group (Fig. 3).[177] Both these mono-*N*-oxide pyridyl amides behaved as nongelators in water; however, stable gelation was achieved for both **1a** and **1b** in the presence of either $ZnCl_2$ or $CdCl_2$ (1 : 2 metal : ligand ratio). Single-crystal X-ray diffraction studies confirmed that while coordination of the metal ions involved the pyridyl nitrogens, the *N*-oxide moieties were engaged in hydrogen bonding with the amide groups in both gels. Although all the metallogels displayed almost similar morphology (needle-type fibrous) under a scanning electron microscope, they behaved differently when exposed to various anions. The anion-responsive nature of the metallogels significantly depends upon the nature of the metal ion present in the gel architecture. While the Zn-gels of both **1a** and **1b** showed multiple responses towards CN^-, F^- and I^-, the Cd-gels of both **1a** and **1b** selectively recognize CN^-

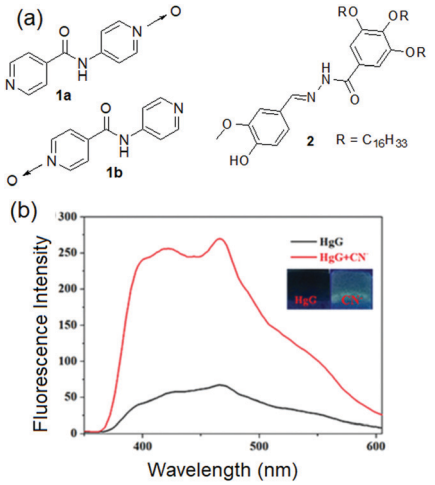

Fig. 3 (a) Chemical structures of compounds **1a**, **1b** and **2**. (b) Change in the emission of the **2**·Hg^{2+} gel (HgG) in the presence of CN^-. The inset presents the color change of the **2**·Hg^{2+} gel (HgG) in the presence of CN^-. Reproduced from ref. 178 with permission from the Royal Society of Chemistry.

ions, exhibiting gel-to-sol transitions. Halides such as F^-, Cl^-, Br^- and I^- did not affect the gel network, whilst CN^-, being a stronger ligand, scavenged the Cd^{2+}-ions, making the gelator molecules free from the polymeric gel network and resulting in sol formation (the concentration of all anions was 2 equiv.).

Unlike compounds **1a** and **1b**, Yin *et al.* reported a compound, **2** (an example of Type II in Fig. 2), which was capable of self-assembling into a stable supramolecular polymer material in DMSO without the assistance of any metal ions.[178] The gel formation was primarily driven by intermolecular hydrogen bonding involving the hydroxyl groups and the van der Waals forces exerted by the long alkyl chains. Such assembled structures were further stabilized by the acylhydrazone group, which locks the molecular conformation by forming intramolecular hydrogen bonding, which in turn facilitates π–π stacking of the phenyl rings. In the structure, the acylhydrazone functionality additionally served as a metal-binding site. Diffusion of Hg^{2+} ions into the gel network resulted in the conversion of the organogel into a **2**·Hg^{2+} metallogel in which the emission of the ligand at 475 nm was almost quenched. The Hg^{2+} ion binding by the acylhydrazone of **2** was confirmed by infrared resonance spectra, which showed shifting of the stretching frequencies at 1583, 3192, and 1639 cm^{-1} for the –C═O, –NH and –C═N groups to 1581, 1641, and 3197 cm^{-1}, respectively. It was proposed that Hg^{2+} binding involving the –C═O, –NH and –C═N groups induced charge transfer and quenched the fluorescence of the Hg-gel. This Hg-gel was further employed in anion sensing involving competitive binding interactions between metal ions, anions, and gelators. Among various anions (F^-, Cl^-, Br^-, I^-, AcO^-, $H_2PO_4^-$, HSO_4^-, N_3^-, SCN^-, S^{2-}, ClO_4^- and CN^-), the Hg-metallogel showed strong yellow fluorescence selectively in the presence of CN^- ions and thereby executed its visual sensing in the gel–gel state (Fig. 3). The gradual addition of CN^- (0–0.8 equiv.) to the **2**·Hg^{2+} gel resulted in demetallation and restoration of the original spectra of organogel **2**. The similar microstructure of the CN^--treated metallogel to the original DMSO gel of **2** again confirmed the CN^--induced demetallation reaction. The detection limit of the **2**·Hg^{2+} gel for CN^- was reported as 3.72×10^{-9} M, quite a lot lower than the standard of the WHO.

It is worth mentioning that acylhydrazones are widely used for synthesizing aggregation-induced fluorescent gels.[93,179–181] The five-membered ring formed by the intramolecular hydrogen bonding of the acylhydrazone locked the molecular conformation in a planar arrangement and enables the aromatic groups to stack with one another in a directional way. Such locking of molecules increases the rigidity and thereby inhibits fluorescence quenching by restricting intramolecular rotation as well as inhibiting photo-induced electron transfer. Consequently, an increase in the gelator concentration shows significant enhancement of the emission of the gel compared to the monomeric solution. Furthermore, a number of metallogels can be prepared from such a self-supported gelator by introducing various metal ions inside the gel network. Depending upon the nature of the metal ions, these metallogels can exhibit various morphology, photophysical properties and anion responsiveness during gel–gel transitions. Such systems are attractive in developing multi analyte optical sensor arrays.[182–185]

Lin *et al.* introduced gelator **3** containing the same acylhydrazone moiety as a cation binder and a quinoline unit as a better aromatic capping group and fluorescence signalling unit than the phenyl of **2** (Fig. 4).[186] The organogel of **3** in DMF showed aggregation-induced strong brilliant blue emission. In the presence of 0.5 equiv. of various metal ions such as Cu^{2+}, Fe^{3+}, Hg^{2+}, and Cr^{3+}, the strong emission at 500 nm was almost quenched and the corresponding non-fluorescent metallogels were obtained. On the other hand, the

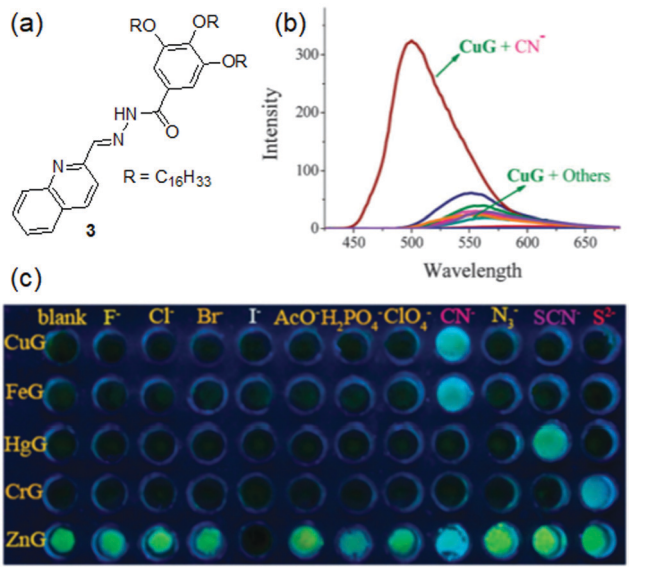

Fig. 4 (a) Structure of gelator **3**. (b) Change in emission of the **3**·Cu^{2+} gel (CuG, 0.8% in DMF) in the presence of CN^- and other anions (F^-, Cl^-, Br^-, I^-, AcO^-, $H_2PO_4^-$, N_3^-, SCN^-, ClO_4^- and S^{2-}). (c) Change in the color of different metallogels in the presence of 1 equiv. of various anions. Reproduced from ref. 186 with permission from the Royal Society of Chemistry.

diffusion of Zn^{2+} ions into the organogel of **3** resulted in an almost 40 nm red shift of the emission spectra and the color of the gel changed to yellow. When the gels were treated with anions, while the **3**·Cu^{2+} and **3**·Fe^{3+} gels selectively responded to CN^- and recognized it *via* fluorescence turn-on, the Hg^{2+} and Cr^{3+}-gels of **3** were non-responsive to the same. Rather they showed fluorescence emission in the presence of SCN^- and S^{2+} ions, respectively. On the other hand, while I^- quenched the strong yellow emission of the **3**·Zn^{2+} gel by the heavy atom effect, CN^- complexation with Zn^{2+} retrieved the original blue color of the gel. Importantly, the **3**·Cu^{2+} and **3**·Fe^{3+} gels could selectively sense CN^- ions from a mixture with other anions (multi-analyte conditions) with limits of detection of 1.0×10^{-7} M and 1.0×10^{-5} M, respectively. Based on these observations, a five-membered sensor array was created which could identify different anions in water with high accuracy and sensitivity. Moreover, these metallogels were explored in the construction of erasable security display materials.

Sun *et al.* undertook a different strategy in developing CN^--responsive gels. They incorporated two different metal ions inside the gel network, so that if CN^- could scavenge one metal ion then the gel state might still persist in the presence of the second metal ion (Fig. 5). They introduced L-glutamic acid Schiff base **4**, which was incapable of forming a gel in a variety of organic solvents (Fig. 6).[187] However, stable yellow and green colored gels were obtained in DMSO either by direct treatment with $Zn(OAc)_2$ and $Cu(OAc)_2$, respectively, or by treating the solutions obtained with $Zn(ClO_4)_2$ and $Cu(ClO_4)_2$ with NaOAc. The Zn·**4** and Cu·**4** metallogels showed different responses under UV-light. While the Zn·**4** gel exhibited strong, brilliant blue fluorescence at 457 nm, the Cu·**4** gel was non-fluorescent. Following these observations, they prepared a green-colored Zn–Cu composite gel (Zn^{2+} : Cu^{2+} : **4** = 1 : 1 : 1) either by adding Cu^{2+} to the Zn·**4** gel or by diffusing Zn^{2+} into the Cu·**4** gel. However, the properties of the Zn–Cu·**4** gels were invariant to the sequence of metal ion addition. The Zn–Cu·**4** gel could recognize CN^- ions with specific selectivity over other anions by exhibiting a naked eye detectable color change from green to yellow, and a change from a non-fluorescent to a blue colored gel under UV-luminescence. In this process, the detection limit of the Zn–Cu·**4** gel for CN^- ions was 1.6×10^{-6} M. From UV-vis, fluorescence, and mass spectra it was confirmed that the properties of the CN^--treated Zn–Cu·**4** gel were identical to

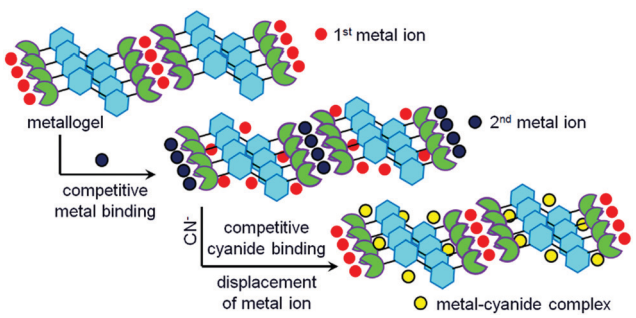

Fig. 5 Cartoon representing the mechanism of cyanide sensing involving a two metal ion composite gel.

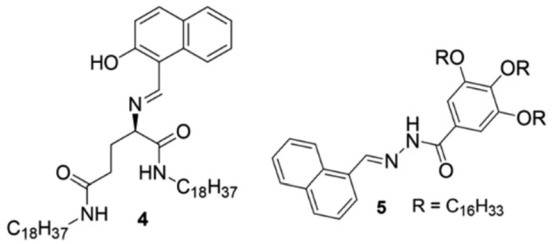

Fig. 6 Structures of compounds **4** and **5**.

those of the original Zn·**4** gel. They suggested that CN^- ions competitively bound to Cu^{2+} to form stable $[Cu(CN)_x]^{n-}$ complexes, while the Zn^{2+} remained coordinated with **4** and maintained the gel structure. Further addition of Cu^{2+} again enabled the restoration of the non-fluorescent Zn–Cu·**4** gel. An off–on–off fluorescence switch was constructed by altering the addition of CN^- and Cu^{2+}, which allowed detection for at least four cycles without any substantial loss of the fluorescence efficiency of the Zn–Cu·**4** gel.

A similar method was followed by Lin *et al.* to explore gelator **5** as a CN^- sensor in gel–gel mode (Fig. 6).[188] Unlike **4**, compound **5** formed stable organogels in various solvents such as dimethyl sulfoxide, propanol, ethanol, *n*-butanol, and iso-amyl alcohol. Among these solvents, **5** showed the highest gel-to-sol transition temperature and lowest minimum gelation concentration (0.4% w/v, 10 mg mL^{-1} = 1%) in ethanol. On the addition of calcium perchlorate to the ethanol gel of **5**, a stable Ca^{2+}-coordinated metallogel was formed, accompanied by strong brilliant blue coloration under UV-light. Initially, they examined the competitive coordination of Ca^{2+}/Cu^{2+} with **5** by adding Cu^{2+} to the Ca-metallogel, which turned the fluorescent Ca-metallogel into a non-fluorescent Ca–Cu-metallogel through replacement of the Ca^{2+} from the acylhydrazone binding core. This Ca–Cu-metallogel showed a selective response for CN^- among various anions by exhibiting turn on emission of the gel. It was suggested that, because of the Group 11 element, Cu^{2+} showed stronger coordination ability with acylhydrazone than that of group 2 element Ca^{2+} and replaced it from the metal binding site. Further addition of CN^- showed higher affinity for Cu^{2+} ions and scavenged them from the acylhydrazone binding core, which allowed Ca^{2+} ions to engage with the acylhydrazone group and restored the brilliant blue emission of the gel.

Metal coordination followed by demetallation using CN^- is apparently an indirect method of sensing where CN^- ions do not interact with the original gelator. Although this could be an effective strategy for CN^- sensing with a very low detection limit, however, the reported systems encountered several drawbacks. The success of such gels considerably depends on many factors such as the self-assembly ability of the gelators in the presence of chemical guests, the role of the metal ions, the nature of the anions taken in the study, the concentration of the chemical analytes, *etc.* Metallogels can show additional interactions with other anions as well. For instance, the Cd-gels of both **1a** and **1b** developed by the Damodaran group, apart from CN^-, also showed a gel-to-sol phase transition in the presence of a very high concentration of I^- (5 equiv.).[177] Hence, these gels are

effective in CN^- sensing only at a low concentration of cyanide. Similarly, the Zn–Cu·**4** metallogel additionally showed interactions with S^{2-} and Cys and recognized them by fluorescence quenching.[187] However, the major issue is that the construction of CN^- responsive metallogels is really very complicated and often relies on trial-and-error methods. For example, gelator **2** was also capable of forming a metallogel with Fe^{3+}. However, unlike the Hg^{2+}-gel, the Fe^{3+}-gel remained silent for CN^- ions but exhibited strong emission with $H_2PO_4^-$.[178] In the same line, gelator **3** reported by Lin *et al.* could form stable gels in the presence of a number of metal ions such as Cu^{2+}, Fe^{3+}, Hg^{2+}, Cr^{3+}, and Zn^{2+}, of which only the **3**·Cu^{2+} and **3**·Fe^{3+} gels showed selective interactions with CN^-.[186] While the **3**·Zn^{2+} gel showed interactions with both CN^- and I^-, the Hg^{2+}·**3** and Cr^{3+}·**3** metallogels were non-interactive with CN^- and showed responses to SCN^- and S^{2-}, respectively. Recently, the same research group introduced compound **6**, which could form a series of organogels in the presence of various metal ions (Fig. 7).[189] Among the metallogels, only the Al–Fe and Al–Cu gels could execute selective visual detection of CN^- by fluorescence turn-on. Other metallogels either remained silent in the presence of cyanide or showed multiple responses with anions. The same is also true for tripodal gelator **7**, for which only the Ni^{2+}-gel behaved as a cyanide sensor (Fig. 7).[190] Further, it is not always true that gels containing the same metal ions would show similar responses towards cyanide. The responsive behavior of these gels entirely depends on the nature of the coordination site and hence the outcome is quite unpredictable. For example, while the Hg^{2+}-gel of **2** validates selective visual sensing of cyanide, the same metallogel of **3** was nonresponsive to CN^-. A similar comparison can be made by considering the contrasting behavior of the Cu^{2+}-metallogels of **3** and **7**. In this context, the detail of cyanide sensing by metal anchored gels is provided in Table 1. Such unpredictable and inconsistent performance makes it complicated and more difficult to design cyanide sensing metallogelators. Hence, there was a real need to consider other approaches for cyanide sensing which allowed design of new molecules that interact directly with cyanide ions either through hydrogen bonding or *via* a chemical reaction.

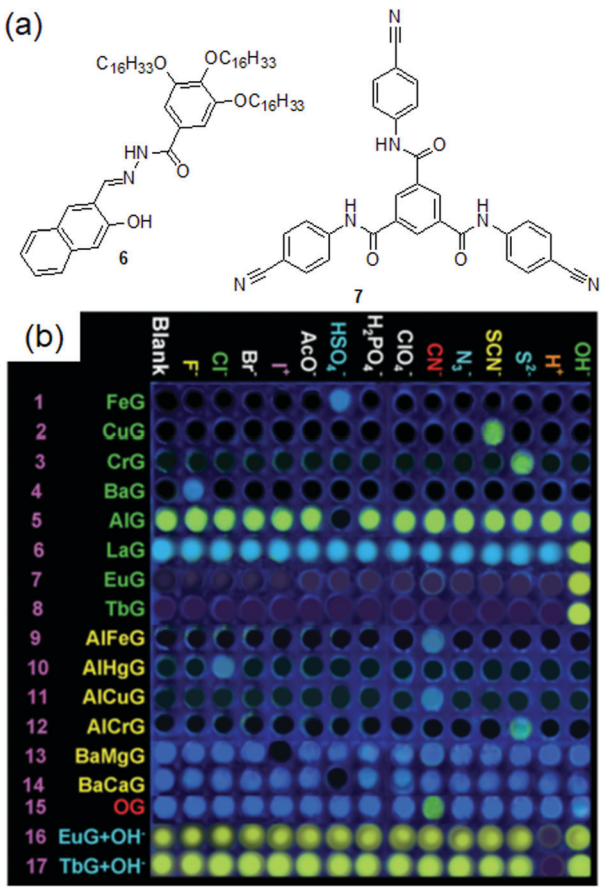

Fig. 7 (a) Structures of compounds **6** and **7**. (b) Gel-based sensor array of metallogels of **6** in the presence of various anions. Reproduced from ref. 189 with permission from the Royal Society of Chemistry.

(ii) H-Bonding motif-based CN^- sensory gels

H-Bonding motif-based cyanide sensory gels typically contain various hydrogen bond donor functionalities such as hydroxyl, amide, sulphonamide, urea, acylhydrazone *etc.* on the gelator skeleton. During the interaction, they can form strong intermolecular hydrogen bonds with the incoming cyanide ions and produce changes in the gel properties (Fig. 8). Again, cyanide sensing can induce either a gel-to-sol or a gel-to-gel phase transformation, which is unpredictable. Hydrogen bonding with CN^- often leads to deprotonation of the corresponding donor hydrogen, which in turn produces optical changes. In order to achieve a better spectroscopic response during the sensing process, the hydrogen bonding groups can be connected directly with aromatic surfaces, so that the effective π-conjugation length can be increased after deprotonation. Apart from the H-bonding core, the rest of the gelator design follows similar approaches as discussed earlier.

Compound **8** is an example of a hydrogen bonding-functionalized cyanide-responsive gelator (Fig. 9), which was capable of forming stable gels in organic solvents like ethylene glycol and benzyl alcohol as well as in a mixture solvent like DMSO/water (8 : 2, v/v).[191] Both the intermolecular H-bonding involving the amide groups and the π–π interactions between the aromatic moieties were responsible for gel formation. The DMSO–water gel was comprised of entangled and twisted fibers of several micrometers as observed by a scanning electron microscope. It could also form a stable gel with CN^- with a fibril structure. The CN^--gel showed lower thermal stability than the original gel of **8**. Hence, the DMSO–water gel of **8** was capable of detecting CN^- ions in a gel–gel fashion by exhibiting a change in the gel properties. However, the gelator simultaneously showed similar changes in the presence of other anions like F^-, AcO^- and $H_2PO_4^-$, and hence the interaction with CN^- was not selective. By correlating proton NMR and solution phase interactions studies, it was suggested that solvation of these anions in the prescribed solvent made it a less efficient competitor for the gelator –NH groups and partly influenced the intermolecular hydrogen bonding so that the gel maintained its structure.

To make the anion–ligand interaction stronger, the sulfonamide group was introduced by Hu *et al.* in designing anion

Table 1 List of metallogels explored in cyanide sensing

Gelator	Sensing mode	Solvent	Metal ion	Selective cyanide sensor	Detection limit (M) (gel)	Response to other anions	Ref.
1a, 1b	Gel-to-sol	Water	Zn^{2+} Cd^{2+}	Zn^{2+} Cd^{2+}	——	(i) Only limited anions are studied (ii) Zn-gel: interference from halides (iii) Cd-gel: interference from I^-	*Supramol. Chem.*, 2020, **32**, 276
2	Gel-to-gel	DMSO	Hg^{2+} Fe^{3+}	Hg^{2+}	3.72×10^{-9}	No interference from other anions Fe-gel: nonresponsive to CN^- but showed interaction with $H_2PO_4^-$	*Soft Matter*, 2019, **15**, 4187
3	Gel-to-gel	DMF	Cu^{2+}, Fe^{3+}, Zn^{2+}, Hg^{2+}, Cr^{3+}	Cu^{2+} Fe^{3+}	1.0×10^{-7} 1.0×10^{-5}	No interference from other anions No interference from other anions Zn-gel: additional response to iodide Hg and Cr gel: no response to cyanide but a response to S^{2-} and Cys	*Chem. Commun.*, 2015, **51**, 1635
4	Gel-to-gel	DMSO	Zn–Cu	—	1.6×10^{-6}	Additional interaction with iodide	*Chem. Commun.*, 2016, **52**, 768
5	Gel-to-gel	EtOH	Cd–Cu	—	1.0×10^{-6}	No interference	*Chem. – Eur. J.*, 2014, **20**, 11457
6	Gel-to-gel	*n*-Butyl alcohol	A number of metal ions	Al^{3+}/Cu^{2+}-gel Al^{3-}/Fe^{3+}-gel	1.0×10^{-7} ——	No interference from other metal ions for the Al^{3+}/Cu^{2+}-gel and Al^{3-}/Fe^{3+}-gel. Other metallogels were insensitive to cyanide	*Chem. Sci.*, 2016, **7**, 5341.
7	Gel-to-gel	DMF–water	Zn^{2+} Ni^{2+} Cu^{2+} Fe^{2+}	Ni-gel	2.2×10^{-7}	No interference Other metallogels were nonresponsive to cyanide but interacts with; Zn-gel: Br^-, Cu-gel: SCN^- Fe-gel: S^{2-}	*Soft Matter*, 2017, **13**, 6243

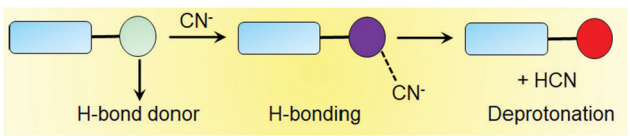

Fig. 8 Mode of interaction of hydrogen bonding motif-based gelators with cyanide.

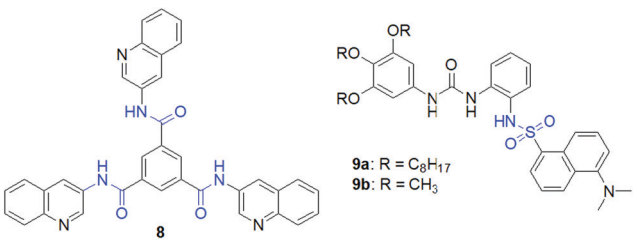

Fig. 9 Structures of compounds **8**, **9a** and **9b**.

responsive gels. They synthesized compound **9a**, which formed a green fluorescent gel in DMSO (Fig. 9).[127] In the structure, they additionally incorporated a urea functionality in close proximity to the sulphonamide to strengthen the ligand–anion interaction through participation in hydrogen bonding. However, initially, the urea group promotes self-aggregation *via* bifurcated hydrogen bonding.[86,192] Furthermore, the non-gelling behavior of **9b** in comparison to **9a** also endorsed the supportive role of hydrophobic interactions in gelation. The response of organogel **9a** towards CN^- led to easy-to-discern changes in the fluorescence color. On exposure to CN^-, the organogel underwent a gel-to-sol transition into a homogeneous non-emissive solution.

Instead of a long alkyl chain, the sulphonamide functionality has been attached to the cholesteryl group to synthesize the gelator. Conceptually, cholesterol with a large hydrophobic surface can stimulate molecular self-assembly *via* hydrophobic interactions.[172–174] Ghosh *et al.* established the cholesterol-appended sulfonyl hydrazone derivative **10** as a naked-eye anionic-sensor (Fig. 10).[128] Employing intermolecular H-bonding involving the sulfonamide moieties and hydrophobic interactions between the cholesterol units, compound **10** formed a stable gel from

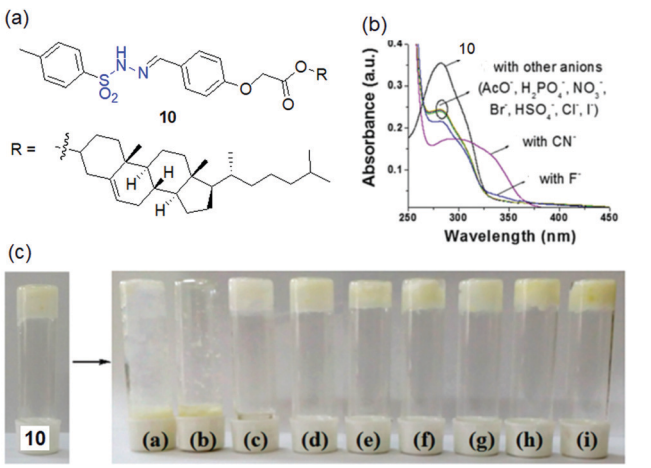

Fig. 10 (a) Chemical structure of gelator **10**. (b) Change in absorbance of **10** [$c = 2.50 \times 10^{-5}$ M, taken in DMSO–H_2O (1 : 1 v/v)] upon addition of 40 equiv. of different anions ($c = 1.0 \times 10^{-3}$ M, taken in DMSO). (c) Visual sensing of cyanide by **10** (c = 20 mg mL^{-1}) in DMSO–H_2O (1 : 1 v/v) involving gel to sol phase transformation: (a) CN^-, (b) F^-, (c) AcO^-, (d) $H_2PO_4^-$, (e) Cl^-, (f) Br^-, (g) I^-, (h) HSO_4^- and (i) NO_3^-. Reproduced from ref. 128 with permission from The Royal Society of Chemistry (RSC) on behalf of the Centre National de la Recherche Scientifique (CNRS) and the RSC.

DMSO–H_2O. The SEM image of the xerogel shows a tiny rod-like fibrous structure in the aggregated state. Among different anions, basic anions like CN^- and F^- interact with the sulfonamide –NH and disrupt the hydrogen bond-assisted molecular aggregation through deprotonation, causing gel-to-sol transformation. Other weakly basic anions were practically non-interfering in such an event. However, a relatively better response was observed for CN^- than F^- ions. The presence of 2 equiv. of CN^- caused the complete destruction of the gel within 30 min, while F^- ions took almost 2 h to bring a similar change. Importantly, in the presence of less than 2 equiv. of F^- the gel was virtually stable, while gel-to-sol transformation was achieved with one equiv. of CN^- ions. Further, to discriminate these two anions, different metal ions (Ca^{2+} and Fe^{3+}) were used as chelating agents. Only Ca^{2+} ions successfully differentiated CN^- from F^- ions. The scavenging of F^- ions by Ca^{2+} ions from the medium retrieved gelation. Compound **10** also exhibited strong interactions with CN^-, showing ratiometric changes in the absorption spectra. Upon successive addition of CN^- ions (up to 40 equiv.), the initial absorption band at 282 nm gradually decreased along with the simultaneous increase of a new absorption band at 330 nm, leading to a clear isosbestic point at 312 nm. For F^- ions, such a ratiometric response was very weak. CN^- ions displayed relatively stronger binding than F^- ions in 1 : 1 stoichiometric fashion (2.12×10^3 M^{-1} and 1.04×10^3 M^{-1} for CN^- and F^- ions, respectively) with a moderate detection limit (7.96×10^{-5} M). As suggested, the F^- ion due to its smaller size was more hydrated in water compared to CN^- and remained less free to interact with gelator **10**, while the CN^- ion being less hydrated could display its basic nature and thereby showed a relatively sharp and better response. Thus, apart from the gel-to-sol conversion of **10** in the presence of CN^- and F^- ions in different time frames, use of Ca^{2+} ions and comparison of absorption spectra and binding constant data were important in discriminating CN^- from F^- ions.

Like sulfonyl hydrazone, acylhydrazones can also interact with anions by hydrogen bonding involving –NH and therefore are utilized in sensor design. The designed gelators **11a** and **11b** differ in boron substitution and therefore showed different self-assembly attributes as well as anion sensing properties (Fig. 11).[193] Compound **11a** being more hydrophilic than **11b** exhibited gelation in the presence of water (acetonitrile–water, 4 : 6, v/v), whilst hydrophobic molecule **11b** self-assembled in a chloroform–methanol (1 : 9, v/v) mixture. In the sensing process, while the gel of **11a** remained intact after the addition of CN^- and F^- ions, the organogel of **11b** turned into a solution in the presence of both the anions. It was explained by the idea that the presence of the two hydroxyl groups on the boron center provides extra stability to the gel by increasing the number of hydrogen bond contacts and thereby prevents the gel from rupturing in the presence of anions. On the contrary, compound **12** showed a rapid gel-to-sol phase transition with CN^- in dioxane (Fig. 11).[194] Strong hydrogen bonding of –NH with CN^- followed by deprotonation broke the yellow gel into a dark orange sol instantly. The gel was retrieved by adding Hg^{2+} ions to the broken gel. Importantly, Hg^{2+} ions scavenge CN^- ions from the medium and allow the molecules to reassemble. However, the recovered gel showed a decrease in mechanical properties.

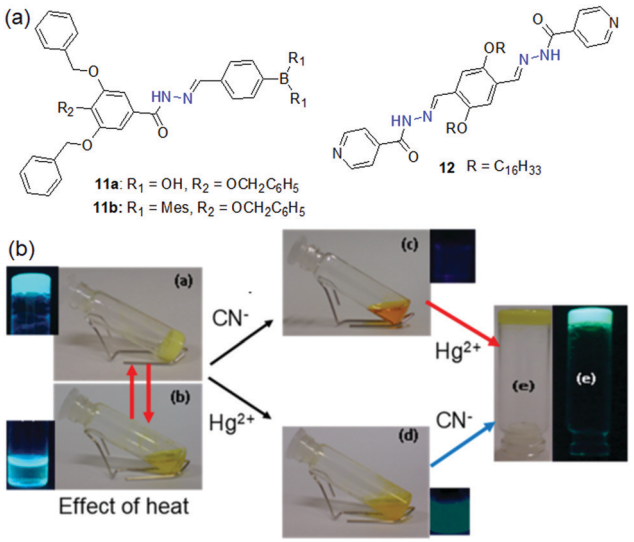

Fig. 11 (a) Structures of compounds **11a**, **11b** and **12**. (b) Sol–gel phase transformation of the dioxane gel of **12** under different conditions. Reproduced with permission from ref. 194. Copyright 2019 American Chemical Society.

Recently, two acylhydrazone derived LMWGs **13** and **14** have been introduced for cyanide sensing (Fig. 12). While compound **13** exhibited a gel-to-sol transition in the presence of cyanide in DMSO : H_2O (1 : 1, v/v) with a color change from white to yellow,[195] the DMF : H_2O (1 : 1, v/v) gel of **14** recognized cyanide ions in a gel-to-gel fashion involving a rapid color change from yellow to saffron.[196] ^1H NMR studies confirmed that both the compounds undergo deprotonation of the acyl hydrazone –NH in the presence of cyanide in semi aqueous medium. Interestingly, the color change of the cyanide treated gel of **14** was reversible in the presence of a proton source, enabling the reusability of the material.

To control the molecular assembly, –OH groups have been incorporated near the acylhydrazone moiety in different ways to achieve structures **15–17**. The –OH group is involved in intramolecular hydrogen bonding with the adjacent imine nitrogen and provides rigidity to the molecules as discussed above. Importantly, in some cases, the six-membered hydrogen-bonded network becomes so stable that it prevents deprotonation

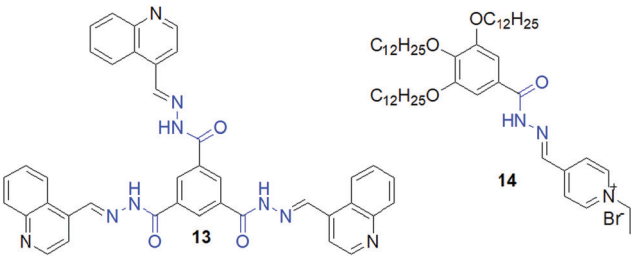

Fig. 12 Structures of compounds **13** and **14**.

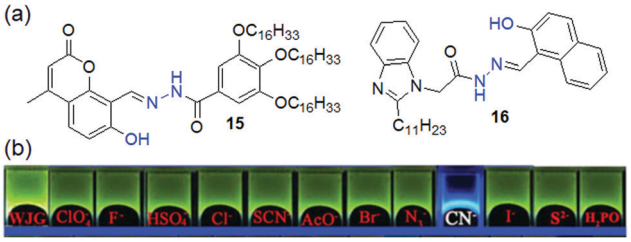

Fig. 13 (a) Structures of compounds **15** and **16**. (b) Fluorescence response of organogel **16** (WJG) to the presence of various anions. Reproduced from ref. 198 with permission from The Royal Society of Chemistry (RSC) on behalf of the Centre National de la Recherche Scientifique (CNRS) and the RSC.

of –OH with anions. Compound **15** is a classic example, which forms a gel in *n*-BuOH/H_2O (9 : 1, v/v) driven by the hydrogen bond-mediated rigidity of the molecules (Fig. 13).[197] The gel, when treated with various anions, underwent a gel-to-gel transition in the presence of CN^- ions, exhibiting blue-shifted emission in the fluorescence spectra. The detection was also confirmed visually through a color change of the gel from green-yellow to blue fluorescence. However, this cyanide sensing suffered from poor selectivity as the gel showed a similar response to S^{2-} as well. Interestingly, by spectroscopic studies, it was corroborated that during interaction with anions, the –OH remained intact while the –NH group underwent deprotonation and produced remarkable spectroscopic changes of the gels. On the other hand, the glycerol gel of **16** undergoes deprotonation of both the phenolic –OH and acylhydrazone –NH with CN^- and shows visual sensing through a color change of the gel from yellow-green to blue (Fig. 13).[198] This color change was associated with a blue shift in the emission of the gel from 516 nm to 498 nm. However, X-ray diffraction pattern analysis of the CN^- treated gel revealed peaks at 2θ = 25.95° and 27.90° corresponding to *d*-spacing of 3.43 Å and 3.19 Å, which indicated that the π–π stacking between the naphthyl rings of **16** and **16**·CN^- was not influenced even after the deprotonation process.

Our group, for the first time, explored a pyridoxal-based LMWG **17** in anion sensing (Fig. 14).[199] Structural analysis revealed that, while several hydrogen bond donor and acceptor entities such as phenolic –OH, alcoholic –OH, amide –NH and pyridyl ring nitrogen assist the molecular assembly through hydrogen bonding, the aryl ether segments are involved in π-stacking. A combination of all these weak forces resulted in the formation of stable gels from various solvents such as DMSO, DMF, DMSO/H_2O, and DMF/H_2O. When the DMSO-gel of **17** was subjected to common basic anions and halides, the gel showed a strong affinity toward basic anions such as F^-, AcO^- and CN^- ions. These anions caused deprotonation of the phenolic –OH and the amide –NH, for which the self-assembly of **17** was destroyed and the gel was completely transformed into a solution in different times (for F^-: 3 h, CN^-: 3.5 h and AcO^-: 6.5 h) according to the basicity of the corresponding anions ($F^- > CN^- > AcO^-$). Regeneration of the gel states after the addition of water to the anion-induced broken gels further supported the deprotonation phenomena. To discriminate F^-, AcO^- and CN^- ions, different chelating agents were introduced

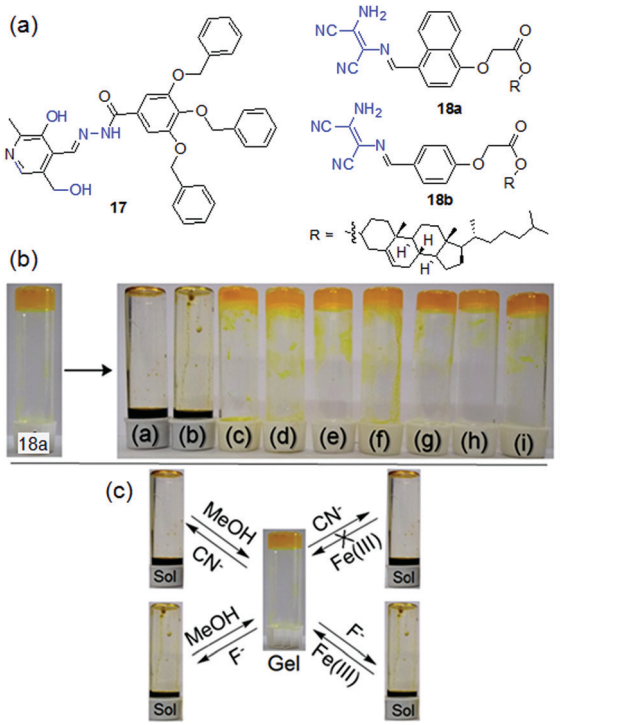

Fig. 14 (a) Structures of compounds **17**, **18a** and **18b**. (b) Phase transformation of **18a** in toluene in the presence of different anions: (a) CN^-, (b) F^-, (c) AcO^-, (d) $H_2PO_4^-$, (e) Cl^-, (f) Br^-, (g) I^-, (h) NO_3^- and (i) HSO_4^-. (c) Chemical reversibility of the anion-induced sols and discrimination between F^- and CN^- ions. Reproduced from ref. 200 with permission from The Royal Society of Chemistry (RSC) on behalf of the Centre National de la Recherche Scientifique (CNRS) and the RSC.

to the anion-induced broken gels. The addition of BF_3 to the broken gels retrieved the gel states in all cases. Addition of $Ca(ClO_4)_2$ could recover the F^--induced broken gel only and thereby differentiate F^- from AcO^- and CN^- ions visually. The use of other chelating agents such as $Cu(ClO_4)_2$ and $AgClO_4$ was also found to be ineffective to differentiate AcO^- and CN^- ions. Hence, gelator **17** acts as a cyanide sensor but with poor selectivity.

Two structurally similar diaminomaleonitrile-based gelators **18a** and **18b** have been recently reported by us as excellent cyanide-indicators where the diaminomaleonitrile core as the anion-binding site was attached to the cholesterol unit *via* an aromatic linker (naphthalene/benzene) (Fig. 14).[200] A small change in the π-surface (naphthalene/benzene) significantly influenced the gelation behaviors and gel properties (mgc, thermal stability, morphology, mechanical behavior, stimuli responsiveness *etc.*). The naphthyl analogue **18a** exhibited gelation in a greater number of solvents compared to the benzene analogue **18b**, while in common solvents **18a** formed a gel with relatively low mgc and improved thermal and mechanical properties. The naphthyl derivative **18a** exhibited self-healing behavior and also acted as an injectable material, while the benzene analog **18b** did not. However, both the compounds showed identical anion-responsiveness. The toluene and 1,2-dichlorobenzene gels of **18a** and **18b** respectively sense F^- and CN^- anions by showing rapid gel-to-sol transformation through

the deprotonation of the diaminomaleonitrile $-NH_2$ group. Other basic anions and halides virtually remained inert to such phase changes and thereby validated the sensing of F^- and CN^- ions. The addition of MeOH to the broken gels recovered gelation with no virtual changes in the gel properties. Importantly, F^- and CN^- ions were distinguished by adding external chelating agents like Fe^{3+} ions to the broken gels where only the scavenging of F^- ions through FeF_6^{3-} formation rendered gelation. Further, in solution (acetonitrile) both the compounds displayed a similar trend and recognized them by exhibiting ratiometric absorption spectral changes with 1 : 1 stoichiometric binding to F^- and CN^- ions.

H-Bonding motif-based gelators are simple in design (Table 2). They are advantageous over metallogels in terms of cost-effectiveness and ease of handling. However, the H-bond mediated detection technique still encounters several limitations. Basic anions like F^-, AcO^-, $H_2PO_4^-$ *etc.* frequently interfere in the sensing process.[128,191,193,194,197,199,200] Interference from basic anions makes this kind of gelators less selective and hence less effective. In many cases, it demands different chelating agents or solvent optimization to show CN^- selectivity for such multi-responsive gels, which makes this strategy a little complicated.[128,200] In some cases, even the chelating agents are inefficient to discriminate CN^- from other anions.[199] These limitations necessitated the development of reaction-based gelators where specific chemical reactions with CN^- ions at the reaction center could minimize the interference of other anions.

In this context, it is mentionable that most of the hydrogen bonding-motif based compounds were subjected to anion binding studies in solution. As in solution molecules remain discrete compared to a gel, solution-phase studies showed different selectivity for anions, and even higher selectivity to cyanide in some cases.[127,128] This indicates that the self-assembly nature of the gelators has a critical role in the responsive behavior.

(iii) Reaction-based CN^- sensory gelators

Cyanide responsive reaction-based gelator probes (dosimetric gelators) differ from the H-bonding motif-based sensors only in the reaction centre (binding site), where instead of reversible hydrogen bonding, cyanide forms a permanent covalent bond (Fig. 15). The rest of the gelator segments follow almost similar design strategies. Dicyanovinyl, oxazole, *etc*. and even an activated imine or carbonyl group can serve as a potential acceptor for cyanide.[134] The higher nucleophilicity of cyanide compared to other anions in some specific solvents provides an advantage to react irreversibly with the organic gelator molecules. Other anions remain silent to these reactions. This makes such gelators significantly superior to other types of gelators in terms of selectivity. Another advantage is their fast response time, which allows real-time monitoring of the sensing processes. Cyanide-induced chemical changes of the gelator substantially alter the self-assembly of the molecules and often induce a gel-to-sol transition. Usually these reaction centers are either part of the chromophoric units or different segments connected to the chromophores and thus, due to permanent chemical modifications, there are always notable spectroscopic changes for characterization.

The design of dosimetric sensors is a fairly new domain of research in gel chemistry. Our group has been dedicatedly working on this topic. We have reported dosimetric probes for Hg^{2+},[201–204] perborate,[205] sulfide,[206] and hydrazine[207] for their selective recognition involving sol-to-gel conversion. In the same line, we have shown with compounds **19** and **20** how the functional group modification of the gelator can lead to cyanide sensing selectively (Fig. 16).[208] Both the compounds were based on a cholesterol-linked phenyl substituent, a

Table 2 List of H-bonding motif-based gelators explored in cyanide sensing

Gelators	Sensing mode	Solvent	Detection limit	Interference from other anions	Ref.
8	Gel-to-gel	DMSO : H_2O (8 : 2, v/v)	—	F^-, AcO^- and $H_2PO_4^-$	*RSC Adv.*, 2016, **6**, 83303.
9	Gel-to-sol	DMSO	**9a**: 0.4×10^{-8} M in CH_3CN–water solution	No other anions taken in the gel study	*Dyes and Pigments*, 2015, **119**, 108.
10	Gel-to-sol	DMSO : H_2O (1 : 1, v/v)	7.96×10^{-5} M in DMSO–water solution	F^-	A. Panja, S. Ghosh, K. Ghosh, *New J. Chem.*, 2019, **43**, 10270.
11a	**11a**: nonresponsive towards CN^-	**11a**: acetonitrile–water mixture (4 : 6, v/v)	—	Only CN^- and F^- taken in the gel study	*ChemistrySelect*, 2016, **1**, 3086.
11b	**11b**: gel to sol	**11b**: chloroform-methanol (1 : 9, v/v)		**11b**: F^-	
12	Gel-to-sol	Dioxane	11.2 ppb in THF	Hg^{2+}, no other anions tested	*ACS Sustainable Chem. Eng.*, 2019, **7**, 12304.
13	Gel-to-sol	DMSO : H_2O (1 : 1, v/v)	1.5 mM (in solution)	No other anions tested	*Soft Matter*, 2020, **16**, 6532.
14	Gel-to-gel	DMF : H_2O (1 : 1, v/v)	0.368 mM (in solution)	No interferance from other anions	*ACS Sustainable Chem. Eng.*, 2020, **8**, 8327.
15	Gel-to-gel	*n*-BuOH/H_2O (9 : 1, v/v)	In gel: 1.64×10^{-8} M	S^{2-}	*Soft Matter*, 2020, **16**, 1029.
16	Gel-to-gel	Glycerol	In gel: 3.02×10^{-6} M	No interferance from other anions	*New J. Chem.*, 2018, **42**, 18059.
17	Gel-to-sol	DMSO	—	F^- and AcO^-	*Tetrahedron Lett.*, 2016, **57**, 5469.
18a	Gel-to-sol	**18a**: toluene	**18a**: 1.4×10^{-5} M in CH_3CN	F^-	*New J. Chem.*, 2020, **44**, 10275.
18b		**18b**: 1,2-dichlorobenzene	**18b**: 1.19×10^{-5} M in CH_3CN		
19	Gel-to-sol	Toluene	—	F^-	*Supramol. Chem*, 2019, **31**, 239.

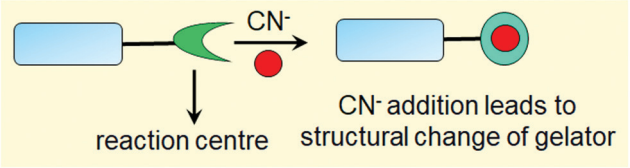

Fig. 15 Mode of interaction of reaction-based gelators with CN^-.

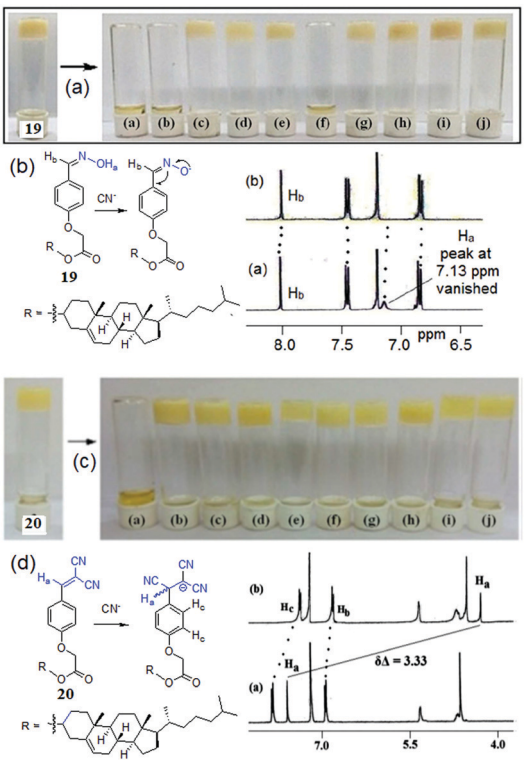

Fig. 16 (a and b) Phase transformation of the organogel of **19** in the presence of various anions along with the proton NMR changes of **19** in the presence of CN^- ions. (c and d) Phase transformation of the organogel of **20** in the presence of various anions along with the proton NMR changes of **20** in the presence of CN^- ions. For (b and d), from left to right: (a) CN^-, (b) F^-, (c) AcO^-, (d) $H_2PO_4^-$, (e) Cl^-, (f) Br^-, (g) I^-, (h) HSO_4^-, (i) CLO_4^- and (j) NO_3^-. Reproduced with permission from ref. 208.

common self-assembling unit. However, while gelator **19** is comprised of an oxime unit as a hydrogen bond donor, gelator **20** possesses a dicyanovinyl moiety as a Michael acceptor for CN^-. The change in functional group in the gelators has a significant impact on the gelation, gel properties, and morphology; however, the main difference lies in their anion sensing behavior. The oxime analogue **19**, due to the free –OH group, interacted with multiple basic anions like CN^-, F^-, and AcO^- and displayed a gel-to-sol transition within 1 h with no selectivity. The phase transitions were attributed to the anion-induced deprotonation of the oxime –OH. In contrast, the dicyanovinylated gelator **20** showed a gel-to-sol transition within 15 min selectively in the presence of CN^- over a series of anions and demonstrated visual sensing. Such a high degree of selectivity was ascribed to the Michael type addition of CN^- to the dicyanovinyl moiety in **20**, which in turn established the

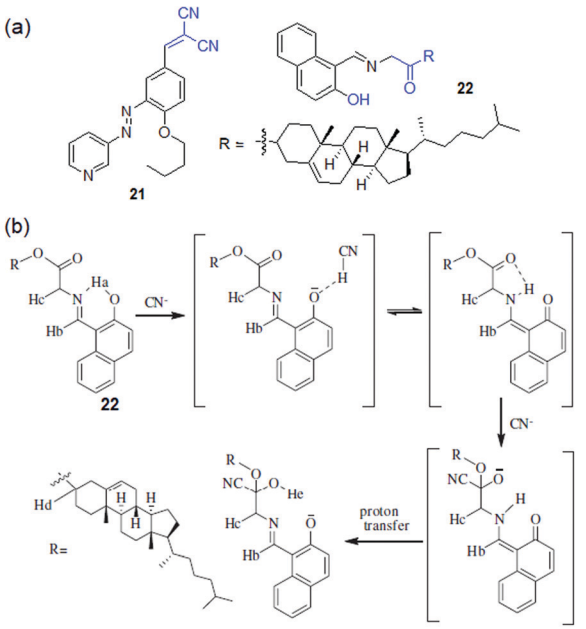

Fig. 17 (a) Structures of compounds **21** and **22**. (b) Probable mechanism of cyanide sensing by **22**. Reproduced with permission from ref. 210.

necessity of designing dosimetric sensors for CN^- ions over hydrogen bonding mediated recognition. The cyanide adduct formation was characterized by proton NMR spectra. In ^1H NMR, the upfield chemical shift of the vinylic proton (Ha) from 7.59 ppm to 4.26 ppm endorsed the nucleophilic addition of CN^- ions to **20**. Similarly, gelator **21** exhibited a selective response to CN^- involving the same chemical reaction and recognized it through the gel-to-sol transition in CH_3CN with a vivid color change from orange-yellow to deep red (a response time of 2 h in the presence of 2 equiv. of cyanide) (Fig. 17).[209] Not only in the gel state, gelators **20** and **21** also showed similar trends in solution and selectively recognized CN^- over other anions by exhibiting ratiometric changes in the absorption spectra.

An activated ester can also serve as a cyanide acceptor. Compound **22** underwent gelation in DMF : H_2O (2 : 1, v/v) through extensive π–π stacking of the naphthalene rings (Fig. 17).[210] The gel was found to be anion-responsive because of the phenolic –OH. CN^- ions over a series of other anions resulted in a rapid gel-to-sol transition (within 8 h) with a colour change from yellow to brown. The sensing mechanism involved cyanide-induced deprotonation of the phenolic –OH followed by nucleophilic addition to the activated ester. ^1H NMR, FTIR, and HRMS studies were conducted to establish CN^- adduct formation *via* nucleophilic addition to the ester carbonyl of **22**.

An interesting feature was observed for gelator **22** in that, unlike **20** and **21**, its selectivity could be controlled in solution either by adjusting its concentration or by changing the solvent composition. A fluorescence study of **22** in CH_3CN containing 1% $CHCl_3$ ($c = 2.5 \times 10^{-5}$ M) enabled the detection of CN^- ions by fluorescence turn-on but it suffered from less selectivity due to interference of F^- and $HP_2O_3^{-7}$. However, an increase in the

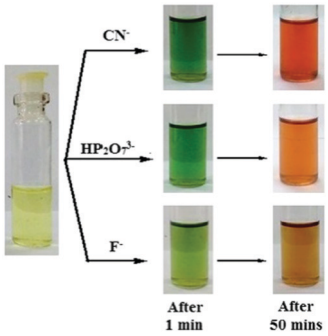

Fig. 18 Photograph showing the colour changes of **22** (c = 1.0 × 10^{-3} M) in the presence of equiv. amounts of various anions (c = 5.0 × 10^{-3} M) with time in CH_3CN containing 4% $CHCl_3$. Adapted with permission from ref. 210.

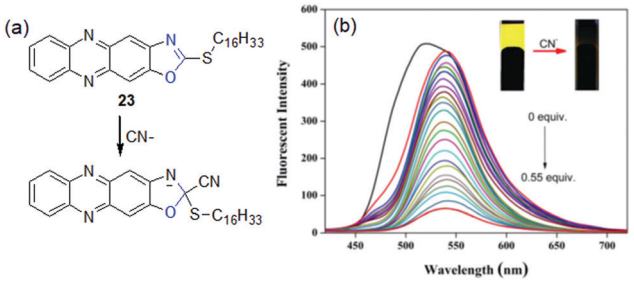

Fig. 19 (a) Chemical reaction involved between **23** and CN^- and (b) change in the emission spectra of the DMSO–water gel of **23** in the presence of increasing amounts of CN^-. The inset presents the corresponding change in the color of the gel. Adapted with permission from ref. 211.

concentration of **22** in solution (c = 1.0 × 10^{-3} M) brought about selectivity towards CN^- with a distinguished colour change of the solution from yellow to rose-red (Fig. 18). It was proposed that initially, due to the presence of large amounts of basic anions, rapid formation of naphthoxide ions favoured excited-state charge transfer, which with time was repressed by the keto–enol equilibrium in solution. Close proximity of –NH of the keto form (Fig. 17b) then triggered CN^- addition to the ester carbonyl of **22** and produced a distinguishable color change from F^- and $HP_2O_7^{3-}$. Similarly, the solution-phase interactions of **22** with the same anions in DMF/H_2O (2 : 1, v/v) showed considerable changes in absorbance and fluorescence selectively to CN^- ions only at higher cyanide concentration, consistent with the gel phase observations.

Despite several advantages, chemodosimetric gelators also have a few drawbacks (Table 3). One major disadvantage of such probes is that the chemical reaction brings about permanent changes of the gelators. As a consequence, the scope for reuse is limited. In some cases, the rate of cyanide addition is very slow at ambient temperature and heating of the gel sample is required to drive the chemical reaction. Fang *et al.* presented 2-(hexadecylthio)oxazolo[4,5-*b*]phenazine **23** as a cyanide sensor (Fig. 19).[211] The phenazine derivative formed a yellow fluorescent gel in DMSO. When aqueous solutions of anions were added to the gel at room temperature, no change in fluorescence was noticed in any case even after a considerable time. However, when the mixtures were heated above the gel melting temperature and then cooled down again, a non-fluorescent gel appeared only for CN^-. At high temperature, CN^- addition to **23** destroyed the π–π interactions, which led to

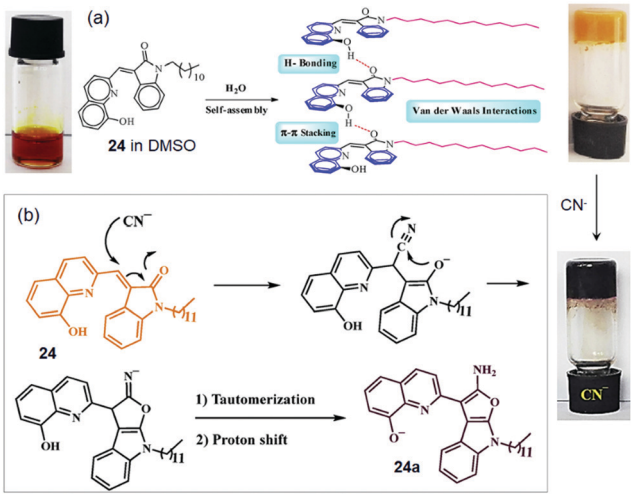

Fig. 20 (a) Suggested self-assembly mechanism for the gel formation of **24** in DMSO/H_2O and (b) a proposed mechanism for the interaction of **24** with CN^-. Reproduced with permission from ref. 212.

steady quenching of the emission during a sol-to-gel transition. The gel showed an extraordinary detection limit of 4.18 × 10^{-10} M for CN^- ions.

In a recent study, supramolecular gelator **24**, composed of indolin-2-one and quinoline moieties with a long chain *N*-alkyl substituted amide group, has been reported to form a stable and durable gel from DMSO/H_2O (1 : 1).[212] The addition of water is explained to enhance the solvophobic interactions, which act as a driving force for the gel (Fig. 20a). The SEM image revealed the closely spaced plate-like morphology of the xerogel. Addition of aqueous solutions of various anions

Table 3 List of reaction-based gelators explored in cyanide sensing

Gelator	Sensing mode	Solvent	Detection limit (M)	Ref.
20	Gel-to-sol	Toluene–CH_3OH (1 : 2, v/v)	4.17 × 10^{-6} (in CH_3CN)	*Supramol. Chem.*, 2019, **31**, 239.
21	Gel-to-sol	CH_3CN	9.36 × 10^{-6} (in CH_3CN)	*ChemistrySelect*, 2018, **3**, 1809.
22	Gel-to-sol	DMF : H_2O (2 : 1, v/v)	1.36 × 10^{-5} (in CH_3CN containing 1% $CHCl_3$)	*Supramol. Chem.*, 2017, **29**, 350.
23	Gel-to-gel	DMSO–water	4.18 × 10^{-10} (gel)	*Dyes and Pigments*, 2020, **174**, 108066
24	Gel-to-gel	DMSO	1.36 × 10^{-4} (in DMSO solution)	*Talanta*, 2020, **219**, 121237

including CN^- as their sodium salts to a DMSO solution of **24** furnished a color change of the gel. In the presence of CN^- ions, the orange colored gel changed into a dark purple color. It was suggested that, at first, compound **24** undergoes a pseudo-Michael attack by CN^- ions, followed by a ring-closing reaction. Subsequent proton shift and tautomerization reactions finally generate the conjugate anion **24a**, responsible for the dark purple color (Fig. 20b). Thus gelator **24** was used as an extremely selective and fast chemosensor for the detection of CN^- ions in environmental water resources.

Conclusions and future outlook

Gel-based sensing probes have huge potential in materials chemistry research.[80–100] This review provides an up-to-date report describing cyanide sensing in the gel phase. Attention has been given to the approaches where the hydrogen bonding and nucleophilic character of cyanide are encountered to show gel-to-sol as well as gel-to-gel phase transformation for its detection and sensing. The solution-phase interactional approaches for cyanide sensing are well-reviewed.[132–139] Indeed, limited gelators are available for cyanide detection. Most of the cyanide-responsive gels are serendipitous. This is probably due to the uncertainty of the responsive behaviour of a molecule, which is an inherent challenge in the field of gel chemistry.[149,213–216] Hence, study of the structure–property relationship of gelators is highly desirable.[217]

Gel-based cyanide sensors are extremely useful, particularly as accessing sophisticated instrumentation and trained manpower is limited. The study so far performed in this domain is mainly connected with the detection of cyanide involving only phase transformation and observable color changes. Other properties like swelling–deswelling *etc.* are not investigated. Polymeric gels have been reported to show changes in gel volume in the presence of cyanide.[218] It would be interesting to see if small molecule gelators respond in a similar way. If the results are positive, it is then possible to construct cyanide responsive actuators. Furthermore, unlike other design-based sensors, low molecular weight gelators are rarely explored in *in vivo* detection of cyanide,[219–221] and hence designing fluorophore tagged gelators is highly demanding for constructing bioimaging probes.[63] As the majority of cyanide sources belong to industrial waste, emphasis should also be put on adsorbing and separating cyanide from cyanide contaminated water. Importantly, although some designed gelators show quite a low detection limit compared to the prescribed limit of the WHO, their sensitivities for cyanide are not so high in most cases. Alongside this, cyanide mostly exists in aqueous systems, while most of the gelators are studied in pure organic solvent. Hence, discovery of super-gelators capable of forming hydrogels at extremely low concentrations is highly essential for improving the sensitivity of detection.

Conflicts of interest

There are no conflicts to declare.

Acknowledgements

SP thanks the University of Glasgow for funding. KG thanks DST, New Delhi, India, for providing facilities in the department under the FIST program. KG also thanks SERB, DST, New Delhi, for financial support in a project (File No. EMR/2016/008005/OC).

References

1 P. Terech and R. G. Weiss, Low Molecular Mass Gelators of Organic Liquids and the Properties of Their Gels, *Chem. Rev.*, 1997, **97**, 3133–3160.
2 R. Weiss and P. Terech, *Molecular Gels: Materials with Self-Assembled Fibrillar Networks*, 2005.
3 L. A. Estroff and A. D. Hamilton, Water Gelation by Small Organic Molecules, *Chem. Rev.*, 2004, **104**, 1201–1218.
4 E. R. Triboni, T. B. F. Moraes and M. J. Politi, in *Nano Design for Smart Gels*, ed. R. Bacani, F. Trindade, M. J. Politi and E. R. Triboni, Elsevier, 2019, pp. 35–69, DOI: 10.1016/B978-0-12-814825-9.00003-5.
5 J.-Y. Zhang, L.-H. Zeng and J. Feng, Dynamic covalent gels assembled from small molecules: from discrete gelators to dynamic covalent polymers, *Chin. Chem. Lett.*, 2017, **28**, 168–183.
6 J. Zhang, Y. Hu and Y. Li, *Gel Chemistry: Interactions, Structures and Properties*, Springer Singapore, Singapore, 2018, pp. 9–59, DOI: 10.1007/978-981-10-6881-2_2.
7 C. J. C. Edwards-Gayle and I. W. Hamley, Self-assembly of bioactive peptides, peptide conjugates, and peptide mimetic materials, *Org. Biomol. Chem.*, 2017, **15**, 5867–5876.
8 P. A. Kollman, Noncovalent interactions, *Acc. Chem. Res.*, 1977, **10**, 365–371.
9 E. R. Johnson, S. Keinan, P. Mori-Sánchez, J. Contreras-García, A. J. Cohen and W. Yang, Revealing Noncovalent Interactions, *J. Am. Chem. Soc.*, 2010, **132**, 6498–6506.
10 V. Bhalla, *Supramol. Chem., Reson.*, 2018, **23**, 277–290.
11 S. S. Babu, V. K. Praveen and A. Ajayaghosh, Functional π-Gelators and Their Applications, *Chem. Rev.*, 2014, **114**, 1973–2129.
12 F. Huang and X. Zhang, Introduction to supra-amphiphiles, *Mater. Chem. Front.*, 2020, **4**, 11.
13 G. Ouyang and M. Liu, Self-assembly of chiral supra-amphiphiles, *Mater. Chem. Front.*, 2020, **4**, 155–167.
14 Y. Wang, J. Chou, Y. Sun, S. Wen, S. Vasilescu and H. Zhang, Supramolecular-based nanofibers, *Mater. Sci. Eng., C*, 2019, **101**, 650–659.
15 G. Vantomme and E. W. Meijer, The construction of supramolecular systems, *Science*, 2019, **363**, 1396–1397.
16 E. R. Draper and D. J. Adams, Low-Molecular-Weight Gels: The State of the Art, *Chem*, 2017, **3**, 390–410.
17 N. M. Sangeetha and U. Maitra, Supramolecular gels: Functions and uses, *Chem. Soc. Rev.*, 2005, **34**, 821–836.
18 C. Creton, 50th Anniversary Perspective: Networks and Gels: Soft but Dynamic and Tough, *Macromolecules*, 2017, **50**, 8297–8316.

19 A. E. Danks, S. R. Hall and Z. Schnepp, The evolution of 'sol–gel' chemistry as a technique for materials synthesis, *Mater. Horiz.*, 2016, **3**, 91–112.
20 Z. Huang, B. Qin, L. Chen, J.-F. Xu, C. F. J. Faul and X. Zhang, Supramolecular Polymerization from Controllable Fabrication to Living Polymerization, *Macromol. Rapid Commun.*, 2017, **38**, 1700312.
21 D. B. Amabilino, D. K. Smith and J. W. Steed, Supramolecular materials, *Chem. Soc. Rev.*, 2017, **46**, 2404–2420.
22 D. K. Smith, *Molecular Gels: Structure and Dynamics*, The Royal Society of Chemistry, 2018, pp. 300–371, DOI: 10.1039/9781788013147-00300.
23 J. Y. C. Lim, S. S. Goh, S. S. Liow, K. Xue and X. J. Loh, Molecular gel sorbent materials for environmental remediation and wastewater treatment, *J. Mater. Chem. A*, 2019, **7**, 18759–18791.
24 A. Dawn, Supramolecular Gel as the Template for Catalysis, Inorganic Superstructure, and Pharmaceutical Crystallization, *Int. J. Mol. Sci.*, 2019, **20**, 781.
25 S. Panja, B. Dietrich and D. J. Adams, Chemically Fuelled Self-Regulating Gel-to-Gel Transition, *ChemSystemsChem*, 2020, **2**, e1900038.
26 H. Chang, C. Li, R. Huang, R. Su, W. Qi and Z. He, Amphiphilic hydrogels for biomedical applications, *J. Mater. Chem. B*, 2019, **7**, 2899–2910.
27 P. K. Hashim, J. Bergueiro, E. W. Meijer and T. Aida, Supramolecular Polymerization: A Conceptual Expansion for Innovative Materials, *Prog. Polym. Sci.*, 2020, **105**, 101250.
28 E. R. Draper and D. J. Adams, Controlling the Assembly and Properties of Low-Molecular-Weight Hydrogelators, *Langmuir*, 2019, **35**, 6506–6521.
29 M. Hartlieb, E. D. H. Mansfield and S. Perrier, A guide to supramolecular polymerizations, *Polym. Chem.*, 2020, **11**, 1083–1110.
30 M. Xiong, C. Wang, G. Zhang and D. Zhang, *Functional Molecular Gels*, The Royal Society of Chemistry, 2014, pp. 67–94, DOI: 10.1039/9781849737371-00067.
31 X. Yu, L. Chen, M. Zhang and T. Yi, Low-molecular-mass gels responding to ultrasound and mechanical stress: towards self-healing materials, *Chem. Soc. Rev.*, 2014, **43**, 5346–5371.
32 H.-J. Schneider, *Chemoresponsive Materials: Stimulation by Chemical and Biological Signals*, The Royal Society of Chemistry, 2015, pp. 1–9, DOI: 10.1039/9781782622420-00001.
33 C. D. Jones and J. W. Steed, Gels with sense: supramolecular materials that respond to heat, light and sound, *Chem. Soc. Rev.*, 2016, **45**, 6546–6596.
34 X. Sui, X. Feng, M. A. Hempenius and G. J. Vancso, Redox active gels: synthesis, structures and applications, *J. Mater. Chem. B*, 2013, **1**, 1658–1672.
35 W. Cheng and Y. Liu, in *Biopolymer-Based Composites*, ed. S. Jana, S. Maiti and S. Jana, Woodhead Publishing, 2017, pp. 31–60, DOI: 10.1016/B978-0-08-101914-6.00002-8.
36 M. J. Taylor, P. Tomlins and T. S. Sahota, Thermoresponsive Gels, *Gels*, 2017, **3**, 4.
37 H. Frisch and P. Besenius, pH-Switchable Self-Assembled Materials, *Macromol. Rapid Commun.*, 2015, **36**, 346–363.
38 R. K. Mishra, S. Das, B. Vedhanarayanan, G. Das, V. K. Praveen and A. Ajayaghosh, *Molecular Gels: Structure and Dynamics*, The Royal Society of Chemistry, 2018, pp. 190–226, DOI: 10.1039/9781788013147-00190.
39 D. Kuckling, Stimuli-Responsive Gels, *Gels*, 2018, **4**, 60.
40 C. Echeverria, S. N. Fernandes, M. H. Godinho, J. P. Borges and P. I. P. Soares, Functional Stimuli-Responsive Gels: Hydrogels and Microgels, *Gels*, 2018, **4**, 54.
41 H. Wu, J. Zheng, A.-L. Kjøniksen, W. Wang, Y. Zhang and J. Ma, Metallogels: Availability, Applicability, and Advanceability, *Adv. Mater.*, 2019, **31**, 1806204.
42 S. Shah, N. Rangaraj, K. Laxmikeshav and S. Sampathi, ''Nanogels as drug carriers – Introduction, chemical aspects, release mechanisms and potential applications'', *Int. J. Pharm.*, 2020, **581**, 119268.
43 X. Yang, G. Zhang and D. Zhang, Stimuli responsive gels based on low molecular weight gelators, *J. Mater. Chem.*, 2012, **22**, 38–50.
44 H.-J. Schneider, *Chemoresponsive Materials: Stimulation by Chemical and Biological Signals*, The Royal Society of Chemistry, 2015, pp. 44–66, DOI: 10.1039/9781782622420-00044.
45 W. Zhang and C. Gao, Morphology transformation of self-assembled organic nanomaterials in aqueous solution induced by stimuli-triggered chemical structure changes, *J. Mater. Chem. A*, 2017, **5**, 16059–16104.
46 Y. Wang, Programmable hydrogels, *Biomaterials*, 2018, **178**, 663–680.
47 E. R. Draper and D. J. Adams, Photoresponsive gelators, *Chem. Commun.*, 2016, **52**, 8196–8206.
48 A. Panja and K. Ghosh, Triazole-amide isosteric pyridine-based supramolecular gelators in metal ion and biothiol sensing with excellent performance in adsorption of heavy metal ions and picric acid from water, *New J. Chem.*, 2019, **43**, 934–945.
49 F. Chen, Y.-M. Wang, W. Guo and X.-B. Yin, Color-tunable lanthanide metal–organic framework gels, *Chem. Sci.*, 2019, **10**, 1644–1650.
50 M. A. Mohamed, A. Fallahi, A. M. A. El-Sokkary, S. Salehi, M. A. Akl, A. Jafari, A. Tamayol, H. Fenniri, A. Khademhosseini, S. T. Andreadis and C. Cheng, Stimuli-responsive hydrogels for manipulation of cell microenvironment: From chemistry to biofabrication technology, *Prog. Polym. Sci.*, 2019, **98**, 101147.
51 T. Shao, N. Falcone and H.-B. Kraatz, Supramolecular Peptide Gels: Influencing Properties by Metal Ion Coordination and Their Wide-Ranging Applications, *ACS Omega*, 2020, **5**, 1312–1317.
52 O. Erol, A. Pantula, W. Liu and D. H. Gracias, Transformer Hydrogels: A Review, *Adv. Mater. Technol.*, 2019, **4**, 1900043.
53 S. Panja and D. J. Adams, Gel to gel transitions by dynamic self-assembly, *Chem. Commun.*, 2019, **55**, 10154–10157.
54 S. Panja, A. M. Fuentes-Caparrós, E. R. Cross, L. Cavalcanti and D. J. Adams, Annealing Supramolecular Gels by a Reaction Relay, *Chem. Mater.*, 2020, **32**, 5264–5271.

55 S. Panja and D. J. Adams, Pathway Dependence in Redox-Driven Metal–Organic Gels, *Chem. – Eur. J.*, 2020, **26**, 6130–6135.
56 Y. Ohsedo, Low-Molecular-Weight Gelators as Base Materials for Ointments, *Gels*, 2016, **2**, 13.
57 J. Puigmartí-Luis and D. B. Amabilino, *Functional Molecular Gels*, The Royal Society of Chemistry, 2014, pp. 195–254, DOI: 10.1039/9781849737371-00195.
58 S. Ghosh, V. K. Praveen and A. Ajayaghosh, The Chemistry and Applications of π-Gels, *Annu. Rev. Mater. Res.*, 2016, **46**, 235–262.
59 W. Fang, Y. Zhang, J. Wu, C. Liu, H. Zhu and T. Tu, Recent Advances in Supramolecular Gels and Catalysis, *Chem. – Asian J.*, 2018, **13**, 712–729.
60 G. R. Deen and X. J. Loh, Stimuli-Responsive Cationic Hydrogels in Drug Delivery Applications, *Gels*, 2018, **4**, 13.
61 J. Li, W.-Y. Wong and X.-m. Tao, Recent advances in soft functional materials: preparation, functions and applications, *Nanoscale*, 2020, **12**, 1281–1306.
62 J. Li, L. Geng, G. Wang, H. Chu and H. Wei, Self-Healable Gels for Use in Wearable Devices, *Chem. Mater.*, 2017, **29**, 8932–8952.
63 N. Mehwish, X. Dou, Y. Zhao and C.-L. Feng, Supramolecular fluorescent hydrogelators as bio-imaging probes, *Mater. Horiz.*, 2019, **6**, 14–44.
64 K. G. Cho, J. I. Lee, S. Lee, K. Hong, M. S. Kang and K. H. Lee, Light-Emitting Devices Based on Electrochemiluminescence Gels, *Adv. Funct. Mater.*, 2020, **30**, 1907936.
65 G. Sharifzadeh and H. Hosseinkhani, Biomolecule-Responsive Hydrogels in Medicine, *Adv. Funct. Mater.*, 2017, **6**, 1700801.
66 P. K. Bolla, V. A. Rodriguez, R. S. Kalhapure, C. S. Kolli, S. Andrews and J. Renukuntla, A review on pH and temperature responsive gels and other less explored drug delivery systems, *J. Drug Delivery Sci. Technol.*, 2018, **46**, 416–435.
67 M. Mauro, Gel-based soft actuators driven by light, *J. Mater. Chem. B*, 2019, **7**, 4234–4242.
68 L. Li, J. M. Scheiger and P. A. Levkin, Design and Applications of Photoresponsive Hydrogels, *Adv. Mater.*, 2019, **31**, 1807333.
69 N. N. Ferreira, L. M. B. Ferreira, V. M. O. Cardoso, F. I. Boni, A. L. R. Souza and M. P. D. Gremião, Recent advances in smart hydrogels for biomedical applications: From self-assembly to functional approaches, *Eur. Polym. J.*, 2018, **99**, 117–133.
70 J. Mayr, C. Saldías and D. Díaz Díaz, Release of small bioactive molecules from physical gels, *Chem. Soc. Rev.*, 2018, **47**, 1484–1515.
71 A. Hong, M.-I. Aguilar, M. P. Del Borgo, C. G. Sobey, B. R. S. Broughton and J. S. Forsythe, Self-assembling injectable peptide hydrogels for emerging treatment of ischemic stroke, *J. Mater. Chem. B*, 2019, **7**, 3927–3943.
72 F. Gao, C. Ruan and W. Liu, High-strength hydrogel-based bioinks, *Mater. Chem. Front.*, 2019, **3**, 1736–1746.
73 Z. Deng, H. Wang, P. X. Ma and B. Guo, Self-healing conductive hydrogels: preparation, properties and applications, *Nanoscale*, 2020, **12**, 1224–1246.
74 Y. Cai, W. Ran, Y. Zhai, J. Wang, C. Zheng, Y. Li and P. Zhang, Recent progress in supramolecular peptide assemblies as virus mimics for cancer immunotherapy, *Biomater. Sci.*, 2020, **8**, 1045–1057.
75 X. Liu, J. Liu, S. Lin and X. Zhao, Hydrogel machines, *Mater. Today*, 2020, **36**, 102–124.
76 J. Zhang and J. Liu, Light-activated nanozymes: catalytic mechanisms and applications, *Nanoscale*, 2020, **12**, 2914–2923.
77 J. Bae, J. Park, S. Kim, H. Cho, H. J. Kim, S. Park and D.-S. Shin, Tailored hydrogels for biosensor applications, *J. Ind. Eng. Chem.*, 2020, **89**, 1–12.
78 X. Hu, J. Karnetzke, M. Fassbender, S. Drücker, S. Bettermann, B. Schroeter, W. Pauer, H. U. Moritz, B. Fiedler, G. Luinstra and I. Smirnova, Smart reactors – Combining stimuli-responsive hydrogels and 3D printing, *Chem. Eng. J.*, 2020, **387**, 123413.
79 J. Hoque, N. Sangaj and S. Varghese, Stimuli-Responsive Supramolecular Hydrogels and Their Applications in Regenerative Medicine, *Macromol. Biosci.*, 2019, **19**, 1800259.
80 F. Fages, Metal Coordination To Assist Molecular Gelation, *Angew. Chem., Int. Ed.*, 2006, **45**, 1680–1682.
81 M.-O. M. Piepenbrock, N. Clarke and J. W. Steed, Metal Ion and Anion-Based ''Tuning'' of a Supramolecular Metallogel, *Langmuir*, 2009, **25**, 8451–8456.
82 G. O. Lloyd and J. W. Steed, Anion-tuning of supramolecular gel properties, *Nat. Chem.*, 2009, **1**, 437–442.
83 M.-O. M. Piepenbrock, G. O. Lloyd, N. Clarke and J. W. Steed, Metal- and Anion-Binding Supramolecular Gels, *Chem. Rev.*, 2010, **110**, 1960–2004.
84 A. J. McConnell, C. S. Wood, P. P. Neelakandan and J. R. Nitschke, Stimuli-Responsive Metal–Ligand Assemblies, *Chem. Rev.*, 2015, **115**, 7729–7793.
85 C. B. Rodell, J. E. Mealy and J. A. Burdick, Supramolecular Guest–Host Interactions for the Preparation of Biomedical Materials, *Bioconjugate Chem.*, 2015, **26**, 2279–2289.
86 J. W. Steed, Anion-tuned supramolecular gels: a natural evolution from urea supramolecular chemistry, *Chem. Soc. Rev.*, 2010, **39**, 3686–3699.
87 M. D. Segarra-Maset, V. J. Nebot, J. F. Miravet and B. Escuder, Control of molecular gelation by chemical stimuli, *Chem. Soc. Rev.*, 2013, **42**, 7086–7098.
88 M. A. Ramin, K. R. Sindhu, A. Appavoo, K. Oumzil, M. W. Grinstaff, O. Chassande and P. Barthélémy, Cation Tuning of Supramolecular Gel Properties: A New Paradigm for Sustained Drug Delivery, *Adv. Mater.*, 2017, **29**, 1605227.
89 H. Maeda, Anion-Responsive Supramolecular Gels, *Chem. – Eur. J.*, 2008, **14**, 11274–11282.
90 T. Tu, W. Fang and Z. Sun, Visual-Size Molecular Recognition Based on Gels, *Adv. Mater.*, 2013, **25**, 5304–5313.
91 C. Ren, J. Zhang, M. Chen and Z. Yang, Self-assembling small molecules for the detection of important analytes, *Chem. Soc. Rev.*, 2014, **43**, 7257–7266.
92 X. Li, Y. Gao and M. J. Serpe, Stimuli-Responsive Assemblies for Sensing Applications, *Gels*, 2016, **2**, 8.

93 M. H. Chua, K. W. Shah, H. Zhou and J. Xu, Recent Advances in Aggregation-Induced Emission Chemosensors for Anion Sensing, *Molecules*, 2019, **24**, 2711.
94 H. Wang, X. Ji, M. Ahmed, F. Huang and J. L. Sessler, Hydrogels for anion removal from water, *J. Mater. Chem. A*, 2019, **7**, 1394–1403.
95 W. P. Singh and R. S. Singh, Gelation-based visual detection of analytes, *Soft Mater.*, 2019, **17**, 93–118.
96 N. Malviya, C. Sonkar, B. K. Kundu and S. Mukhopadhyay, Discotic Organic Gelators in Ion Sensing, Metallogel Formation, and Bioinspired Catalysis, *Langmuir*, 2018, **34**, 11575–11585.
97 Y. Hwang, J. Y. Park, O. S. Kwon, S. Joo, C.-S. Lee and J. Bae, Incorporation of hydrogel as a sensing medium for recycle of sensing material in chemical sensors, *Appl. Surf. Sci.*, 2018, **429**, 258–263.
98 P. A. Gale and C. Caltagirone, Anion sensing by small molecules and molecular ensembles, *Chem. Soc. Rev.*, 2015, **44**, 4212–4227.
99 D. Men, H. Zhang and Y. Li, in *Responsive Nanomaterials for Sustainable Applications*, ed. Z. Sun and T. Liao, Springer International Publishing, Cham, 2020, pp. 165–196, DOI: 10.1007/978-3-030-39994-8_5.
100 S. Panja and K. Ghosh, Progress in Benzimidazole/Benzimidazolium-derived Supramolecular Gelators in Ion Recognition, *Mini-Rev. Org. Chem.*, 2020, DOI: 10.2174/1570193X17999200430090415.
101 M. P. Coughlan, Cyanide in Biology. B. Vennesland, E. E. Conn, C. J. Knowles, J. Westley, F. Wissing, *Q. Rev. Biol.*, 1983, **58**, 143.
102 C. J. Knowles and A. W. Bunch, in *Advances in Microbial Physiology*, ed. A. H. Rose and D. W. Tempest, Academic Press, 1986, vol. 27, pp. 73–111.
103 T. B. Hendry-Hofer, P. C. Ng, A. E. Witeof, S. B. Mahon, M. Brenner, G. R. Boss and V. S. Bebarta, A Review on Ingested Cyanide: Risks, Clinical Presentation, Diagnostics, and Treatment Challenges, *J. Med. Toxicol.*, 2019, **15**, 128–133.
104 R. Eisler and S. N. Wiemeyer, in *Reviews of Environmental Contamination and Toxicology*, ed. G. W. Ware, Springer New York, New York, NY, 2004, pp. 21–54, DOI: 10.1007/978-1-4419-9100-3_2.
105 D. A. Purser and J. L. McAllister, in *SFPE Handbook of Fire Protection Engineering*, ed. M. J. Hurley, D. Gottuk, J. R. Hall, K. Harada, E. Kuligowski, M. Puchovsky, J. Torero, J. M. Watts and C. Wieczorek, Springer New York, New York, NY, 2016, pp. 2308–2428, DOI: 10.1007/978-1-4939-2565-0_63.
106 C. Blumer and D. Haas, Mechanism, regulation, and ecological role of bacterial cyanide biosynthesis, *Arch. Microbiol.*, 2000, **173**, 170–177.
107 D. T. Thompson, Cyanide: Social, industrial and economic aspects, *Gold Bull.*, 2001, **34**, 133.
108 E. Antonini, M. Brunori, G. C. Rotilio, C. Greenwood and B. G. MalmstrÖM, The Interaction of Cyanide with Cytochrome Oxidase, *Eur. J. Biochem.*, 1971, **23**, 396–400.
109 H. Ikegaya, H. Iwase, K. Hatanaka, K. Sakurada, K.-i. Yoshida and T. Takatori, Diagnosis of cyanide intoxication by measurement of cytochrome *c* oxidase activity, *Toxicol. Lett.*, 2001, **119**, 117–123.
110 V. Schulz, Clin. Pharmacokinet. of Nitroprusside, Cyanide, Thiosulphate and Thiocyanate, *Clin. Pharmacokinet.*, 1984, **9**, 239–251.
111 R. Takano, The treatment of leprosy with cyanocuprol, *J. Exp. Med.*, 1916, **24**, 207–211.
112 D. Shan, C. Mousty and S. Cosnier, Subnanomolar Cyanide Detection at Polyphenol Oxidase/Clay Biosensors, *Anal. Chem.*, 2004, **76**, 178–183.
113 Z. Dai, J. Lee and W. Zhang, Chiroptical Switches: Applications in Sensing and Catalysis, *Molecules*, 2012, **17**, 1247–1277.
114 Z. S. do Monte and C. S. Ramos, Development and Validation of a Method for the Analysis of Paroxetine HCl by Circular Dichroism, *Chirality*, 2013, **25**, 211–214.
115 Y. Y. Lee, R. M. Kim, S. W. Im, M. Balamurugan and K. T. Nam, Plasmonic metamaterials for chiral sensing applications, *Nanoscale*, 2020, **12**, 58–66.
116 J. W. Canary, Z. Dai and S. Mortezaei, in *Comprehensive Chirality*, ed. E. M. Carreira and H. Yamamoto, Elsevier, Amsterdam, 2012, pp. 600–624, DOI: 10.1016/B978-0-08-095167-6.00850-8.
117 J. Canary and X. Duan, *Reference Module in Chemistry, Molecular Sciences and Chemical Engineering*, Elsevier, 2016, DOI: 10.1016/B978-0-12-409547-2.12666-6.
118 S. M. Oja, B. Feldman and M. W. Eshoo, Method for Low Nanomolar Concentration Analyte Sensing Using Electrochemical Enzymatic Biosensors, *Anal. Chem.*, 2018, **90**, 1536–1541.
119 G. Gauglitz, Analytical evaluation of sensor measurements, *Anal. Bioanal. Chem.*, 2018, **410**, 5–13.
120 J. Homola, H. Vaisocherová, J. Dostálek and M. Piliarik, Multi-analyte surface plasmon resonance biosensing, *Methods*, 2005, **37**, 26–36.
121 C. McDonagh, C. S. Burke and B. D. MacCraith, Optical Chemical Sensors, *Chem. Rev.*, 2008, **108**, 400–422.
122 Y. Song, W. Wei and X. Qu, Colorimetric Biosensing Using Smart Materials, *Adv. Mater.*, 2011, **23**, 4215–4236.
123 A. Roda, M. Mirasoli, E. Michelini, M. Di Fusco, M. Zangheri, L. Cevenini, B. Roda and P. Simoni, Progress in chemical luminescence-based biosensors: A critical review, *Biosens. Bioelectron.*, 2016, **76**, 164–179.
124 D. Pasini and A. Nitti, Recent Advances in Sensing Using Atropoisomeric Molecular Receptors, *Chirality*, 2016, **28**, 116–123.
125 S. Chen, Y.-L. Yu and J.-H. Wang, Inner filter effect-based fluorescent sensing systems: A review, *Anal. Chim. Acta*, 2018, **999**, 13–26.
126 J. Sun, Y. Lu, L. He, J. Pang, F. Yang and Y. Liu, Colorimetric sensor array based on gold nanoparticles: Design principles and recent advances, *TrAC-Trend, Anal. Chem.*, 2020, **122**, 115754.
127 F. Hu, M. Cao, J. Huang, Z. Chen, D. Wu, Z. Xu, S. H. Liu and J. Yin, Sulfonamide and urea-based anions chemosensors, *Dyes Pigm.*, 2015, **119**, 108–115.

128 A. Panja, S. Ghosh and K. Ghosh, A sulfonyl hydrazone cholesterol conjugate: gelation, anion interaction and its application in dye adsorption, *New J. Chem.*, 2019, **43**, 10270–10277.

129 S. Panja, S. Bhattacharya and K. Ghosh, Pyridine coupled mono and bisbenzimidazoles as supramolecular gelators: selective metal ion sensing and ionic conductivity, *Mater. Chem. Front.*, 2018, **2**, 385–395.

130 S. Panja, S. Mondal, S. Ghosh, U. Ghosh and K. Ghosh, Effect of Substitution at Amine Functionality of 2,6-Diaminopyridine-Coupled Rhodamine on Metal-Ion Interaction and Self-Assembly, *ACS Omega*, 2020, **5**, 13984–13993.

131 K. Ghosh and S. Panja, Cholesterol–based Bisamides on Biphenyl Backbone: A Case of Selective Visual Sensing of F− and H2PO4− through Breaking and Making of Gels, *ChemistrySelect*, 2016, **1**, 3667–3674.

132 J. Ma and P. K. Dasgupta, Recent developments in cyanide detection: A review, *Anal. Chim. Acta*, 2010, **673**, 117–125.

133 Y. H. Lee, O. Y. Kweon, H. Kim, J. H. Yoo, S. G. Han and J. H. Oh, Recent advances in organic sensors for health self-monitoring systems, *J. Mater. Chem. C*, 2018, **6**, 8569–8612.

134 P. B. Pati, Organic chemodosimeter for cyanide: A nucleophilic approach, *Sens. Actuators, B*, 2016, **222**, 374–390.

135 K. Kaur, R. Saini, A. Kumar, V. Luxami, N. Kaur, P. Singh and S. Kumar, Chemodosimeters: An approach for detection and estimation of biologically and medically relevant metal ions, anions and thiols, *Coord. Chem. Rev.*, 2012, **256**, 1992–2028.

136 E. P. Randviir and C. E. Banks, The latest developments in quantifying cyanide and hydrogen cyanide, *TrAC, Trends Anal. Chem.*, 2015, **64**, 75–85.

137 A. Bencini and V. Lippolis, Metal-based optical chemosensors for CN− detection, *Environ. Sci. Pollut. Res.*, 2016, **23**, 24451–24475.

138 D. Udhayakumari, Chromogenic and fluorogenic chemosensors for lethal cyanide ion. A comprehensive review of the year 2016, *Sens. Actuators, B*, 2018, **259**, 1022–1057.

139 F. Wang, L. Wang, X. Chen and J. Yoon, Recent progress in the development of fluorometric and colorimetric chemosensors for detection of cyanide ions, *Chem. Soc. Rev.*, 2014, **43**, 4312–4324.

140 S. Panja, A. P. Chattopadhyay and K. Ghosh, Naphthalene and pyrrole substituted guanidine in selective sensing of Cu^{2+}, Hg^{2+}, Pb^{2+} and CN^{-} ions under different conditions, *Supramol. Chem.*, 2017, **29**, 528–535.

141 C. Rao, Z. Wang, Z. Li, L. Chen, C. Fu, T. Zhu, X. Chen, Z. Wang and C. Liu, Pyridine-hydrazone-controlled cyanide detection in aqueous media and solid-state: tuning the excited-state intramolecular proton transfer (ESIPT) fluorescence modulated by intramolecular NH···Br hydrogen bonding, *Analyst*, 2020, **145**, 1062–1068.

142 J.-b. Zeng, Y.-y. Cao, J.-j. Chen, X.-d. Wang, J.-f. Yu, B.-b. Yu, Z.-f. Yan and X. Chen, Au@Ag core/shell nanoparticles as colorimetric probes for cyanide sensing, *Nanoscale*, 2014, **6**, 9939–9943.

143 P. Jayasudha, R. Manivannan and K. P. Elango, A diquinone–imidazole ensemble for selective colorimetric sensing of cyanide in aqueous medium via anion induced NIR absorption, *RSC Adv.*, 2016, **6**, 25473–25479.

144 P. Raja Lakshmi, R. Manivannan, P. Jayasudha and K. P. Elango, An ICT-based chemodosimeter for selective dual channel sensing of cyanide in an aqueous solution, *Anal. Methods*, 2018, **10**, 2368–2375.

145 R. Dalapati, S. Nandi and S. Biswas, Post-synthetic modification of a metal–organic framework with a chemodosimeter for the rapid detection of lethal cyanide via dual emission, *Dalton Trans.*, 2020, **49**, 8684–8692.

146 S. Manickam and S. K. Iyer, Highly sensitive turn-off fluorescent detection of cyanide in aqueous medium using dicyanovinyl-substituted phenanthridine fluorophore, *RSC Adv.*, 2020, **10**, 11791–11799.

147 S. Naha, S.-P. Wu and S. Velmathi, Naphthalimide based smart sensor for CN^{-}/Fe^{3+} and H_2S. Synthesis and application in RAW264.7 cells and zebrafish imaging, *RSC Adv.*, 2020, **10**, 8751–8759.

148 R. Koch, Y. Sun, A. Orthaber, A. J. Pierik and F. Pammer, Turn-on fluorescence sensors based on dynamic intramolecular N → B-coordination, *Org. Chem. Front.*, 2020, **7**, 1437–1452.

149 P. Dastidar, Supramolecular gelling agents: can they be designed?, *Chem. Soc. Rev.*, 2008, **37**, 2699–2715.

150 J.-L. Li and X.-Y. Liu, Architecture of Supramolecular Soft Functional Materials: From Understanding to Micro-/Nanoscale Engineering, *Adv. Funct. Mater.*, 2010, **20**, 3196–3216.

151 N.-B. Lin, Y.-H. Lin, Q.-L. Huang and X.-Y. Liu, Supramolecular gels and mesoscopic structure, *Int. J. Mod. Phys. B*, 2018, **32**, 1840015.

152 M. Liu, G. Ouyang, D. Niu and Y. Sang, Supramolecular gelatons: towards the design of molecular gels, *Org. Chem. Front.*, 2018, **5**, 2885–2900.

153 D. M. Zurcher and A. J. McNeil, Tools for Identifying Gelator Scaffolds and Solvents, *J. Org. Chem.*, 2015, **80**, 2473–2478.

154 A. Dasgupta and D. Das, Designer Peptide Amphiphiles: Self-Assembly to Applications, *Langmuir*, 2019, **35**, 10704–10724.

155 J. A. McCune, S. Mommer, C. C. Parkins and O. A. Scherman, Design Principles for Aqueous Interactive Materials: Lessons from Small Molecules and Stimuli-Responsive Systems, *Adv. Mater.*, 2020, **32**, 1906890.

156 R. Eelkema and A. Pich, Pros and Cons: Supramolecular or Macromolecular: What Is Best for Functional Hydrogels with Advanced Properties?, *Adv. Mater.*, 2020, **32**, 1906012.

157 K. Ariga, M. Nishikawa, T. Mori, J. Takeya, L. K. Shrestha and J. P. Hill, Self-assembly as a key player for materials nanoarchitectonics, *Sci. Technol. Adv. Mater.*, 2019, **20**, 51–95.

158 R. Van Lommel, J. Zhao, W. M. De Borggraeve, F. De Proft and M. Alonso, Molecular dynamics based descriptors for predicting supramolecular gelation, *Chem. Sci.*, 2020, **11**, 4226–4238.

159 Philip A. Gale, Ethan N. W. Howe and X. Wu, Anion Receptor Chemistry, *Chem*, 2016, **1**, 351–422.

160 K. Ghosh and S. Panja, Coumarin-based supramolecular gelator: a case of selective detection of F^- and HP2O73$^-$, *RSC Adv.*, 2015, **5**, 12094–12099.
161 K. Ghosh, D. Kar, S. Panja and S. Bhattacharya, Ion conducting cholesterol appended pyridinium bisamide-based gel for the selective detection of Ag^+ and Cl^- ions, *RSC Adv.*, 2014, **4**, 3798–3803.
162 H. T. Chifotides and K. R. Dunbar, Anion–π Interactions in Supramolecular Architectures, *Acc. Chem. Res.*, 2013, **46**, 894–906.
163 N. Busschaert, C. Caltagirone, W. Van Rossom and P. A. Gale, Applications of Supramolecular Anion Recognition, *Chem. Rev.*, 2015, **115**, 8038–8155.
164 A. Panja and K. Ghosh, Azo and imine functionalized 2-naphthols: promising supramolecular gelators for selective detection of Fe^{3+} and Cu^{2+}, reactive oxygen species and halides, *Mater. Chem. Front.*, 2018, **2**, 1866–1875.
165 S. Mondal, S. Das and A. K. Nandi, A review on recent advances in polymer and peptide hydrogels, *Soft Matter*, 2020, **16**, 1404–1454.
166 Y. Wang, W. Zhang, C. Gong, B. Liu, Y. Li, L. Wang, Z. Su and G. Wei, Recent advances in the fabrication, functionalization, and bioapplications of peptide hydrogels, *Soft Matter*, 2020, DOI: 10.1039/D0SM00966K.
167 T. Ding, F. Tang, G. Ni, J. Liu, H. Zhao and Q. Chen, The development of isoguanosine: from discovery, synthesis, and modification to supramolecular structures and potential applications, *RSC Adv.*, 2020, **10**, 6223–6248.
168 A. Rasines Mazo, S. Allison-Logan, F. Karimi, N. J.-A. Chan, W. Qiu, W. Duan, N. M. O'Brien-Simpson and G. G. Qiao, Ring opening polymerization of α-amino acids: advances in synthesis, architecture and applications of polypeptides and their hybrids, *Chem. Soc. Rev.*, 2020, **49**, 4737–4834.
169 L. Cai, S. Liu, J. Guo and Y.-G. Jia, Polypeptide-based self-healing hydrogels: Design and biomedical applications, *Acta Biomater.*, 2020, **113**, 84–100.
170 A. Dasgupta and D. Das, Designer Peptide Amphiphiles: Self-Assembly to Applications, *Langmuir*, 2019, **35**, 10704–10724.
171 M. Sahranavard, A. Zamanian, F. Ghorbani and M. H. Shahrezaee, A critical review on three dimensional-printed chitosan hydrogels for development of tissue engineering, *Bioprinting*, 2020, **17**, e00063.
172 H. M. T. Albuquerque, C. M. M. Santos and A. M. S. Silva, Cholesterol-Based Compounds: Recent Advances in Synthesis and Applications, *Molecules*, 2019, **24**, 116.
173 H. Svobodová, V. Noponen, E. Kolehmainen and E. Sievänen, Recent advances in steroidal supramolecular gels, *RSC Adv.*, 2012, **2**, 4985–5007.
174 R. Kuosmanen, K. Rissanen and E. Sievänen, Steroidal supramolecular metallogels, *Chem. Soc. Rev.*, 2020, **49**, 1977–1998.
175 S. Panja, S. Ghosh and K. Ghosh, Pyridine/pyridinium symmetrical bisamides as functional materials: aggregation, selective sensing and drug release, *New J. Chem.*, 2018, **42**, 6488–6497.
176 A. Panja and K. Ghosh, Cholesterol-based diazine derivative: selective sensing of Ag+ and Fe3+ ions through gelation and the performance of metallogels in dye and picric acid adsorption from water, *Mater. Chem. Front.*, 2018, **2**, 2286–2296.
177 D. Ghosh, Deepa and K. K. Damodaran, Metal complexation induced supramolecular gels for the detection of cyanide in water, *Supramol. Chem.*, 2020, **32**, 276–286.
178 Z.-Y. Yin, J.-H. Hu, Q.-Q. Fu, K. Gui and Y. Yao, A novel long-alkyl-chained acylhydrazone-based supramolecular polymer gel for the ultrasensitive detection and separation of multianalytes, *Soft Matter*, 2019, **15**, 4187–4191.
179 J. Mei, N. L. C. Leung, R. T. K. Kwok, J. W. Y. Lam and B. Z. Tang, Aggregation-Induced Emission: Together We Shine, United We Soar!, *Chem. Rev.*, 2015, **115**, 11718–11940.
180 E. R. Jimenez and H. Rodríguez, Aggregation-induced emission: a review of promising cyano-functionalized AIE-gens, *J. Mater. Sci.*, 2020, **55**, 1366–1387.
181 Z. Zhao, H. Zhang, J. W. Y. Lam and B. Z. Tang, Aggregation-Induced Emission: New Vistas at the Aggregate Level, *Angew. Chem., Int. Ed.*, 2020, **59**, 9888–9907.
182 J. P. Anzenbacher, P. Lubal, P. Buček, M. A. Palacios and M. E. Kozelkova, A practical approach to optical cross-reactive sensor arrays, *Chem. Soc. Rev.*, 2010, **39**, 3954–3979.
183 K. J. Johnson and S. L. Rose-Pehrsson, Sensor Array Design for Complex Sensing Tasks, *Annu. Rev. Anal. Chem.*, 2015, **8**, 287–310.
184 M. J. Kangas, R. M. Burks, J. Atwater, R. M. Lukowicz, P. Williams and A. E. Holmes, Colorimetric Sensor Arrays for the Detection and Identification of Chemical Weapons and Explosives, *Crit. Rev. Anal. Chem.*, 2017, **47**, 138–153.
185 Z. Li, J. R. Askim and K. S. Suslick, The Optoelectronic Nose: Colorimetric and Fluorometric Sensor Arrays, *Chem. Rev.*, 2019, **119**, 231–292.
186 Q. Lin, T.-T. Lu, X. Zhu, B. Sun, Q.-P. Yang, T.-B. Wei and Y.-M. Zhang, A novel supramolecular metallogel-based high-resolution anion sensor array, *Chem. Commun.*, 2015, **51**, 1635–1638.
187 J. Sun, Y. Liu, L. Jin, T. Chen and B. Yin, Coordination-induced gelation of an l-glutamic acid Schiff base derivative: the anion effect and cyanide-specific selectivity, *Chem. Commun.*, 2016, **52**, 768–771.
188 Q. Lin, B. Sun, Q.-P. Yang, Y.-P. Fu, X. Zhu, T.-B. Wei and Y.-M. Zhang, Double Metal Ions Competitively Control the Guest-Sensing Process: A Facile Approach to Stimuli-Responsive Supramolecular Gels, *Chem. – Eur. J.*, 2014, **20**, 11457–11462.
189 Q. Lin, T.-T. Lu, X. Zhu, T.-B. Wei, H. Li and Y.-M. Zhang, Rationally introduce multi-competitive binding interactions in supramolecular gels: a simple and efficient approach to develop multi-analyte sensor array, *Chem. Sci.*, 2016, **7**, 5341–5346.
190 N. Malviya, M. Das, P. Mandal and S. Mukhopadhyay, A smart organic gel template as metal cation and inorganic anion sensor, *Soft Matter*, 2017, **13**, 6243–6249.

191 A. Ghosh, P. Das, R. Kaushik, K. K. Damodaran and D. A. Jose, Anion responsive and morphology tunable tripodal gelators, *RSC Adv.*, 2016, **6**, 83303–83311.
192 K. Ghosh, S. Panja and S. Bhattacharya, Naphthalene linked pyridyl urea as a supramolecular gelator: a new insight into naked eye detection of I− in the gel state with semiconducting behaviour, *RSC Adv.*, 2015, **5**, 72772–72779.
193 P. Malakar, C. Arivazhagan, M. G. Chowdhury, S. Ghosh and E. Prasad, Poly(Aryl Ether) based Borogels: A New Class of Materials for Hosting Nanoparticles and Sensing Anions, *ChemistrySelect*, 2016, **1**, 3086–3090.
194 S. K. Samanta, N. Dey, N. Kumari, D. Biswakarma and S. Bhattacharya, Multimodal Ion Sensing by Structurally Simple Pyridine-End Oligo *p*-Phenylenevinylenes for Sustainable Detection of Toxic Industrial Waste, *ACS Sustainable Chem. Eng.*, 2019, **7**, 12304–12314.
195 S. Sharma, M. Kumari and N. Singh, A C3-symmetrical tripodal acylhydrazone organogelator for the selective recognition of cyanide ions in the gel and solution phases: practical applications in food samples, *Soft Matter*, 2020, **16**, 6532–6538.
196 B. Sarkar, P. Prabakaran, E. Prasad and R. L. Gardas, Pyridine Appended Poly(Alkyl Ether) Based Ionogels for Naked Eye Detection of Cyanide Ions: A Metal-Free Approach, *ACS Sustainable Chem. Eng.*, 2020, **8**, 8327–8337.
197 J.-H. Hu, Z.-Y. Yin, K. Gui, Q.-Q. Fu, Y. Yao, X.-M. Fu and H.-X. Liu, A novel supramolecular polymer gel-based long-alkyl-chain-functionalized coumarin acylhydrazone for the sequential detection and separation of toxic ions, *Soft Matter*, 2020, **16**, 1029–1033.
198 H. Yao, J. Wang, S.-S. Song, Y.-Q. Fan, X.-W. Guan, Q. Zhou, T.-B. Wei, Q. Lin and Y.-M. Zhang, A novel supramolecular AIE gel acts as a multi-analyte sensor array, *New J. Chem.*, 2018, **42**, 18059–18065.
199 K. Ghosh and C. Pati, Aryl ethers coupled pyridoxal as supramolecular gelator for selective sensing of F^-, *Tetrahedron Lett.*, 2016, **57**, 5469–5474.
200 R. Raza, A. Panja and K. Ghosh, Diaminomaleonitrile-functionalized gelators in F^-/CN^- sensing, phase-selective gelation, oil spill recovery and dye removal from water, *New J. Chem.*, 2020, **44**, 10275–10285.
201 A. Panja and K. Ghosh, Selective sensing of Hg^{2+} *via* sol–gel transformation of a cholesterol-based compound, *Supramol. Chem.*, 2018, **30**, 722–729.
202 S. Ghosh, A. Panja and K. Ghosh, Selective Dosimetric Sensing of Hg^{2+} Ions by Design-Based Small Molecular Gelator, *ChemistrySelect*, 2020, **5**, 5099–5108.
203 R. Raza, N. Dey, A. Panja and K. Ghosh, Pyridyl Azo-Based Progelator in Selective Sensing of Hg^{2+} and Ag^+ Ions *via* Sol to Gel Conversion, *ChemistrySelect*, 2019, **4**, 11564–11571.
204 A. Panja and K. Ghosh, 4-Hydroxybenzaldehyde derived Schiff base gelators: case of the sustainability or rupturing of imine bonds towards the selective sensing of Ag^+ and Hg^{2+} ions *via* sol–gel methodology, *New J. Chem.*, 2019, **43**, 5139–5149.
205 A. Panja and K. Ghosh, Pyridyl Azo-Based Naphthyl Acetate for Sensing of Hydrazine and Perborate in Sol-Gel Medium, *ChemistrySelect*, 2018, **3**, 9448–9453.
206 R. Raza, A. Panja, M. Mukherjee, P. Chattopadhyay and K. Ghosh, Dosimetric Chromogenic Probe for Selective Detection of Sulfide via Sol–Gel Methodology, *ACS Omega*, 2018, **3**, 17319–17325.
207 A. Panja and K. Ghosh, Diaminomalenonitrile-decorated cholesterol-based supramolecular gelator: aggregation, multiple analyte (hydrazine, Hg^{2+} and Cu^{2+}) detection and dye adsorption, *New J. Chem.*, 2018, **42**, 13718–13725.
208 A. Panja and K. Ghosh, Cholesterol-based simple supramolecular gelators: an approach to selective sensing of CN− ion with application in dye adsorption, *Supramol. Chem.*, 2019, **31**, 239–250.
209 A. Panja and K. Ghosh, Pyridylazo Derivatives with Dicyanovinyl Appendage in Selective Sensing of CN^- in Sol-Gel Medium, *ChemistrySelect*, 2018, **3**, 1809–1814.
210 K. Ghosh and S. Panja, Naphthalene-cholesterol conjugate as simple gelator for selective sensing of CN^- ion, *Supramol. Chem.*, 2017, **29**, 350–359.
211 H. Fang, W.-J. Qu, H.-H. Yang, J.-X. He, H. Yao, Q. Lin, T.-B. Wei and Y.-M. Zhang, A self-assembled supramolecular gel constructed by phenazine derivative and its application in ultrasensitive detection of cyanide, *Dyes Pigm.*, 2020, **174**, 108066.
212 F. Mandegani, H. Zali-Boeini, Z. Khayat and R. Scopelliti, A smart low molecular weight gelator for the triple detection of copper(II), mercury(II), and cyanide ions in water resources, *Talanta*, 2020, **219**, 121237.
213 N. Zweep and J. H. van Esch, *Functional Molecular Gels*, The Royal Society of Chemistry, 2014, pp. 1–29, DOI: 10.1039/9781849737371-00001.
214 R. G. Weiss, The Past, Present, and Future of Molecular Gels. What Is the Status of the Field, and Where Is It Going?, *J. Am. Chem. Soc.*, 2014, **136**, 7519–7530.
215 P. Dastidar, Designing Supramolecular Gelators: Challenges, Frustrations, and Hopes, *Gels*, 2019, **5**, 15.
216 R. G. Weiss, *Molecular Gels: Structure and Dynamics*, The Royal Society of Chemistry, 2018, pp. 1–27, DOI: 10.1039/9781788013147-00001.
217 J. Y. C. Lim, S. S. Goh and X. J. Loh, Bottom-Up Engineering of Responsive Hydrogel Materials for Molecular Detection and Biosensing, *ACS Mater. Lett.*, 2020, 918–950, DOI: 10.1021/acsmaterialslett.0c00204.
218 S. Ha, J. Lee, K.-s. Kim, E. J. Choi, P. Nhem and C. Song, Anion-Responsive Thiourea-Based Gel Actuator, *Chem. Mater.*, 2019, **31**, 5735–5741.
219 L. Hou, F. Li, J. Guo, X. Zhang, X. Kong, X. T. Cui, C. Dong, Y. Wang and S. Shuang, A colorimetric and ratiometric fluorescent probe for cyanide sensing in aqueous media and live cells, *J. Mater. Chem. B*, 2019, **7**, 4620–4629.
220 J. Chao, Z. Li, Y. Zhang, F. Huo, C. Yin, H. Tong and Y. Liu, A ratiometric fluorescence probe for monitoring cyanide ion in live cells, *Sens. Actuators, B*, 2016, **228**, 192–199.
221 L. Long, M. Huang, N. Wang, Y. Wu, K. Wang, A. Gong, Z. Zhang and J. L. Sessler, A Mitochondria-Specific Fluorescent Probe for Visualizing Endogenous Hydrogen Cyanide Fluctuations in Neurons, *J. Am. Chem. Soc.*, 2018, **140**, 1870–1875.

